HHS Public Access

Author manuscript

Circ Res. Author manuscript; available in PMC 2016 July 03.

Published in final edited form as:

Circ Res. 2015 July 3; 117(2): 142–156. doi:10.1161/CIRCRESAHA.117.306712.

Vascular Smooth Muscle LRP6 Limits Arteriosclerotic Calcification in Diabetic LDLR-/- Mice by Restraining Noncanonical Wnt Signals

Su-Li Cheng[1], **Bindu Ramachandran**[1], **Abraham Behrmann**[1], **Jian-Su Shao**[2], **Megan Mead**[1], **Carolyn Smith**[1], **Karen Krchma**[3], **Yoanna Bello Arredondo**[1], **Attila Kovacs**[3], **Kapil Kapoor**[1], **Laurence M. Brill**[1], **Ranjan Perera**[1], **Bart O. Williams**[4], and **Dwight A. Towler**[1]

[1]Diabetes and Obesity Research Center, Sanford-Burnham Medical Research Institute, Orlando, FL 32827

[2]M.D. Anderson Cancer Center, Houston, TX 77030

[3]Washington University, St. Louis, MO 63110

[4]Van Andel Research Institute, Grand Rapids, MI 49503

Abstract

Rationale—Wnt signaling regulates key aspects of diabetic vascular disease.

Objective—We generated *SM22-Cre;LRP6(fl/fl);LDLR-/-* mice to determine contributions of Wnt co-receptor LRP6 in the vascular smooth muscle lineage (VSM) of male LDLR-null mice, a background susceptible to diet (HFD) - induced diabetic arteriosclerosis.

Methods and Results—As compared to *LRP6(fl/fl);LDLR-/-* controls, *SM22-Cre;LRP6(fl/fl);LDLR-/-* (LRP6-VKO) siblings exhibited increased aortic calcification on HFD without changes in fasting glucose, lipids, or body composition. Pulse wave velocity (index of arterial stiffness) was also increased. Vascular calcification paralleled enhanced aortic osteochondrogenic programs and circulating osteopontin (OPN), a matricellular regulator of arteriosclerosis. Survey of ligands and Frizzled (Fzd) receptor profiles in LRP6-VKO revealed upregulation of canonical and noncanonical Wnts alongside Fzd10. Fzd10 stimulated noncanonical signaling and *OPN* promoter activity via an USF-activated cognate inhibited by LRP6. RNAi revealed that USF1 but not USF2 supports *OPN* expression in LRP6-VKO VSM, and immunoprecipitation confirmed increased USF1 association with *OPN* chromatin. ML141, an antagonist of cdc42/Rac1 noncanonical signaling, inhibited USF1 activation, osteochondrogenic programs, alkaline phosphatase, and VSM calcification. Mass spectrometry identified LRP6 binding to protein arginine methyltransferase (PRMT) - 1, and nuclear asymmetric dimethylarginine modification was increased with LRP6-VKO. RNAi demonstrated that PRMT1 inhibits *OPN* and *TNAP* while PRMT4 supports expression. USF1 complexes containing the H3R17Me2a signature of PRMT4

Address correspondence to: Dr. Dwight A. Towler, Sanford-Burnham Medical Research Institute, 6400 Sanger Road, Orlando, FL 32827, Tel: 407-745-2147, dtowler@sanfordburnham.org.

S-L.C., B.R., and A.B. contributed equally to this study.

DISCLOSURES

D.A.T. consulted for Daiichi-Sankyo. B.O.W. consulted for Amgen, and received grant support from Genentech.

are increased with LRP6-VKO. *Jmjd6*, a demethylase downregulated with LRP6 deficiency, inhibits *OPN* and *TNAP* expression, USF1:H3R17Me2a complex formation and transactivation.

Conclusions—LRP6 restrains VSM noncanonical signals that promote osteochondrogenic differentiation, mediated in part via USF1- and arginine methylation – dependent relays.

Keywords

Vascular calcification; LRP6; Wnt; USF1; protein arginine methylation; arteriosclerosis; type 2 diabetes mellitus; transcriptional regulation; signal transduction

INTRODUCTION

Hyperglycemia, hyperlipidemia, and uremia accelerate vascular aging, compromising arterial function necessary for normal blood flow, metabolism and tissue homeostasis[1]. Along with hypertension these dysmetabolic states induce arteriosclerotic stiffening, thereby reducing vascular compliance that underlies Windkessel physiology -- elasticity of conduit vessels that ensures smooth distal tissue perfusion throughout the cardiac cycle[1]. Atherosclerotic burden, mural thickening and fibrosis, medial calcification, elastin fragmentation, non-enzymatic matrix crosslinking, and endothelial dysfunction are features of arteriosclerotic aging. Multiple labs have now identified bone morphogenetic proteins (BMPs) and Wnts – polypeptides that convey paracrine cues during skeletal morphogenesis – as pathogenic signals in arteriosclerotic calcification[2–7]. In studies of LDLR-/- mice fed high fat diabetogenic[8] diets (HFD) typical of western societies, we identified that osteogenic *Msx-Wnt* signaling cascades are ectopically activated in the vasculature with concomitant induction of diabetes[8], obesity, and arterial calcification[5]. Expression of the osteoblast transcription factor *Msx2* in mural myofibroblasts was shown to be activated by inflammatory signals that support arterial mineralization[2, 5]. Conditional deletion of *Msx2* and *Msx1* in the vascular smooth muscle and myofibroblast (VSM) lineage reduces arteriosclerotic calcification and vascular stiffening, with down-regulation of multiple Wnt ligands conveying canonical and noncanonical actions, including *Wnt7b*, *Wnt5a*, and *Wnt2* [9]. In the mesenchymal lineage, Wnt7b induces osteogenesis via both pathways[10, 11]. Intriguingly, when expressed in the endothelial cell (EC) lineage, Wnt7b stabilizes the EC phenotype and thereby restrains mesenchymal expression of *Msx2*[10]. While Wnt16 limits chondroid programing of VSM[6], Wnt5a promotes osteochondral differentiation[4]. Thus, Wnt signals emerge as important contributors to vascular disease biology.

The panoply of Wnt receptors regulating vascular sclerosis is only beginning to be investigated. In broad terms, the 10 members of the Frizzled (Fzd) family of Wnt receptors form complexes with either (a) LDL receptor related proteins LRP5 and LRP6[12]; or (b) other signaling proteins (ROR2, Celsr)[13] to activate canonical or noncanonical signaling pathways, respectively. Additionally, LRP5 stimulates aerobic glycolysis through pathways independent of canonical β-catenin mechanisms[14], and Aaronson introduced the notion that LRP6 could restrain noncanonical cascades[15]. Rajamannan demonstrated that LRP5 supports valve calcification in the apolipoprotein E-null mouse[16]. While LRP5 and LRP6 exhibit redundant roles during prenatal skeletal development[17], human genetics suggest that

LRP6 might play a uniquely important role in postnatal atherosclerosis and osteoporosis[18] and bone-vascular interactions[19].

To better understand the role of the vascular LRP6 Wnt receptor in arteriosclerosis, we utilized the SM22-Cre transgene[20] to delete VSM LRP6[21] in LDLR-/- mice. We discover that LRP6 restrains noncanonical signals that drive VSM osteochondrogenic programs in male LDLR-/- mice fed HFD[8, 9], mediated in part via USF1- and protein arginine methylation- dependent relays.

METHODS

See online Supplement.

RESULTS

Conditional deletion of LRP6 in VSM accentuates aortic calcification in LDLR-/- mice fed HFD, increases vessel stiffening and promotes ectopic arterial expression of the osteochondrogenic phenotype

LRP6 is expressed in the arterial vasculature[22], primarily in mural VSM and fibrous caps of atherosclerotic lesions in the aortic sinus of LDLR-/- mice fed HFD (Figure 1A, 1B; Online Supplement Figures I–II). To better understand the role for LRP6 in the biology of arteriosclerotic calcification, we generated SM22-Cre;LRP6(fl/fl);LDLR-/- mice, conditionally depleting LRP6 in the VSM lineage in male LDLR-null mice, a background susceptible to HFD – induced diabetes and arteriosclerotic calcification[23]. As shown in Figure 1B, following a 3 month challenge with HFD, arterial calcification was increased in SM22-Cre;LRP6(fl/fl);LDLR-/- mice as compared to LRP6(fl/fl);LDLR-/- sibling controls, with calcium deposition observed in both medial and atherosclerotic venues (Supplement Figure III). Chow-fed animals exhibited much lower aortic calcium levels that did not differ between genotypes (Figure 1B). Aortic stiffness was increased in SM22-Cre;LRP6(fl/fl);LDLR-/- mice and by HFD as determined by echocardiography[9] (Figure 1C; reduced aortic arch distensibility); insulin resistance was diet-dependent but independent of genotype (Figure 1D). RT-qPCR analysis revealed reductions in aortic *LRP6* mRNA in SM22-Cre;LRP6(fl/fl);LDLR-/- mice, with concomitant increases in *LRP4* and markers of osteochondrogenic programming (Figure 1E). *Axin2* – a target of canonical β-catenin[24] – was diminished in aortas deficient for LRP6, while *Klf5* – a target of noncanonical Wnt signaling like *OPN*[25, 26] -- was upregulated along with the progenitor marker *Sca1* [27](Fig. 1E). While clear trends for increased aortic osteochondrogenic programming were noted in chow-fed mice with VSM LRP6 deficiency, these differences did not reach significance (Figure IV) in the absence of HFD. However, the increases in osteochondrogenic programs were robustly elaborated in primary aortic VSM cultures from SM22-Cre;LRP6(fl/fl);LDLR-/- mice (Figure 1F; *TNAP, OCN, OPN*) and associated with increased mineralization *in vitro* (vide infra). Aspects of the contractile VSM program were diminished, indicated by down-regulation of *Myh11* and *myocardin* (Figure 1F, and not shown). Plasma levels of osteopontin (OPN)[28] were also increased in SM22-Cre;LRP6(fl/fl);LDLR-/- mice vs. LRP6(fl/fl);LDLR-/- controls following HFD challenge (Figure 1G). Measurement of medial thickness in the ascending aorta sinus revealed no significant

increases in HFD-fed animals with reduced VSM LRP6 although pulse wave velocity was increased (Figure V). Aortic proliferation indices did not differ between genotypes; however, cultured VSM from SM22-Cre;LRP6(fl/fl);LDLR-/- mice exhibited 10% greater BrdU incorporation (Figure VI-VIII). Aortic lumen diameter of animal on HFD did not differ between genotypes as quantified by echocardiography (Figure IX); however, a non-significant trend ($p = 0.1$) for increased Mac2(+) atheroma area in the sinus was observed along with significantly increased thoracic aortic *F4/80* and *IL12A* macrophage expression (Figures X–XI). Importantly, differences in aortic calcification and stiffness between genotypes arose in the absence of differences in HFD-induced changes in fasting blood glucose, lipids, insulin resistance, or body composition (Figures XII–XIII). Thus, absence of VSM LRP6 increases aortic calcification and vascular stiffness in diabetic LDLR-/- mice, and enhances vascular elaboration of an osteochondrogenic gene program.

Wnt ligands and Fzd receptors capable of activating noncanonical signals are upregulated in aortic tissues of SM22-Cre;LRP6(fl/fl);LDLR-/- mice on HFD

Skeletal biomineralization occurs via the overlapping yet distinct mechanisms of membranous (type 1 collagen-oriented) and endochondral (type 10 collagen-oriented) ossification[29]. Canonical Wnt signals promote initiation of the former[17] and inhibit bone resorption[30], while noncanonical Wnt signals promote mature tissue calcification via both mechanisms[31, 32]. LRP6 can restrain noncanonical signals in part by sequestering certain Fzd co-receptors[15]. To assess whether paracrine relays capable of noncanonical signaling were altered in aortic tissues with LRP6 deficiency, we surveyed the expression of *Wnt* ligands and *Fzd* co-receptors. Array analysis of aortic RNA from mice on HFD for 3 months (n= 5/genotype) revealed upregulation of genes encoding multiple *Wnt* ligands and *Fzd10* (Supplement Figure XIV). This was confirmed by RT-qPCR; as compared to LRP6(fl/fl);LDLR-/- controls, SM22-Cre;LRP6(fl/fl);LDLR-/- mice on HFD exhibited elevated levels of *Wnt7b*, *Wnt4*, *Wnt10a*, *Wnt3a*, and *Fzd10* (Figure 2A and Figure 2B). Increases in aortic mRNAs observed *in vivo* required HFD challenge (Figure XV). However, significant upregulation of ligands and *Fzd10* expression was observed in primary VSM cultures (Figure XVI; and vide infra). *Wnt5a* -- the abundant noncanonical agonist[4] -- remained unchanged. Immunohistochemistry and western blot analysis of primary VSM cultures confirmed upregulation of Wnt7b (Figure 2C), Wnt10a (Figure 2D), and Fzd10 protein with down-regulation of LRP6 (Figure 2E). Of note, while Wnt3a and Wnt10a are reported to elicit only canonical signals, Wnt4[33, 34] and Wnt7b[11, 23] are capable of supporting both canonical and noncanonical pathways. Thus, loss of VSM LRP6 leads to the upregulation of Wnt ligands capable of supporting canonical and noncanonical signaling.

Fzd10 activates noncanonical signaling that is inhibited by LRP6 expression, and promotes OPN transcription via USF protein-DNA interactions

Fzd10 activation in sarcoma elicits noncanonical signals[35] similar to Fzd9 in bone[31]. To confirm and extend this, we transiently co-transfected Fzd10 expression vectors with NFAT-LUC[36] and LEF-LUC[23] reporters that register noncanonical and canonical signaling, respectively, in HEK293T cells[37]. As shown in Figure 3A, Fzd10 upregulated NFAT-LUC activity with modest impact on LEF-LUC, while LRP6 upregulated canonical LEF-LUC activity with little effect on NFAT-LUC. However, co-expression of LRP6 reduced Fzd10

activation of NFAT-LUC, and Fzd10 impaired LRP6 upregulation of LEF-LUC (Figure 3A). Similar responses occur with Fzd9 (Figure 3B, and data not shown), the Fzd member most closely related to Fzd10. ML141 – an inhibitor of cdc42/Rac1 signaling[38] in the noncanonical Wnt planar cell polarity pathway[39] – inhibited Fzd10 and Fzd9 activation of NFAT-LUC (Figure 3B). Conversely, constitutively active Cdc42(Q61L) activated NFAT-LUC, and was inhibited by LRP6 (Figure 3C). In primary cultures of aortic VSM, Fzd10 but not Fzd9 is upregulated with LRP6 deficiency (Figure XVI). Furthermore, HEK reporter cells transfected with NFAT-LUC +/- pCMV-Fzd10 exhibited Fzd10-dependent noncanonical NFAT activation when co-cultured onto VSM feeder cell layers from SM22-Cre;LRP6(fl/fl);LDLR-/- mice vs. LRP6(fl/fl);LDLR-/- controls (Figure 3D). This indicated that Fzd10 conveys responsiveness to a noncanonical agonist elaborated by SM22-Cre;LRP6(fl/fl);LDLR-/- VSM.

OPN is an endogenous noncanonical Wnt target[40] and osteochondrogenic gene active during membranous and endochondral bone formation[29], and is upregulated in SM22-Cre;LRP6(fl/fl);LDLR-/- VSM. RNAi targeting *Fzd10* but not *Fzd9* reduces *OPN* gene expression in SM22-Cre;LRP6(fl/fl);LDLR-/- VSM (Figure 4A). As with NFAT-LUC, Fzd10 upregulates *OPN* promoter activity and is inhibited by LRP6 expression (Figure 4B). Unlike Fzd10, Fzd7 and Fzd1 are inactive in this assay (Figure XVII and not shown). Co-expression of either Wnt7b or Wnt5a enhanced Fzd10 activation, while Wnt11 and Wnt4 did not (Figure XVIII). *OPN* promoter mapping identified that the glucose-responsive USF cognate[41] at −80 to −72 relative to the transcriptional start site is required for Fzd10 induction (Figure 4C). Co-expression of either USF1 or USF2 activated the *OPN* promoter, and was inhibited by LRP6 expression (Figure 4D), indicating that *OPN* expression was entrained to noncanonical signals conveyed in part by USF and inhibited by LRP6. Consistent with this, siRNA targeting *USF1*, but not *USF2*, inhibited the upregulation of *OPN* with LRP6 deficiency (Figure 4E; Figure XIX), and chromatin immunoprecipitation revealed increased association of USF1 with *OPN* chromatin in LRP6-deficient VSM (Figure 4F). ML141 inhibited USF1 activation of OPNLUC (Figure 4G) as well as Fzd10 activation of NFAT-LUC (Figure 3B) and OPNLUC (Figure XX). The constitutively active variant Cdc42(Q61L) upregulated the OPN promoter in HEK cells (Figure XXI). Moreover, ML141 reduced *OPN* elevation in LRP6-deficient VSM (Figure 4H); by contrast, the selective Rac1 inhibitor EHT1864[42] exerted little if any effect on *OPN* expression (Figure 4H). Thus, Fzd10- and USF1- activation of the *OPN* promoter is inhibited by LRP6, with LRP6 actions phenocopied by ML141 treatment.

LRP6 associates with PRMT1, and SM22-Cre;LRP6(fl/fl);LDLR-/- aortic VSM exhibits increased nuclear protein ADMA accumulation

To better understand the mechanisms whereby LRP6 regulates signaling, we expressed FLAG-epitope tagged LRP6 in HEK cells, immunoprecipitated FLAG-containing complexes under non-denaturing conditions, and began to characterize the LRP6 interactome by mass spectrometry (to be presented elsewhere). As compared to control cells, immune complexes from LRP6-FLAG expressing cells revealed enrichment of PRMT1. Co-immunoprecipitation of recombinant PRMT1 variant 1 (PRMT1v1) and LRP6-FLAG was independently demonstrated as shown in Figure 5A. PRMT1 is a protein arginine

methyltransferase that catalyzes formation of asymmetric dimethylarginine (ADMA) on protein targets. Consistent with prior reports[43], we identified that PRMT1v1 is present in cytoplasmic, membrane, and nuclear fractions of VSM by western blot analysis and immunohistochemistry (Figure 5B; Figure XXII). PRMT1v2, possessing a nuclear export sequence[43], is only found in the non-nuclear fractions (Figure 5B). These observations prompted assessment of the cellular ADMA profile by western blot. As shown in Figure 5B, protein ADMA modification profiles were altered in the cytoplasmic, membrane, and nuclear fractions of SM22-Cre;LRP6(fl/fl);LDLR-/- VSM; the greatest changes observed were increases in a subset of ADMA-modified nuclear proteins (Figure 5B). Independent assessment of replicates demonstrated ~2- to 3 -fold increases in specific nuclear ADMA – modified proteins (Figures 5C and 5D).

PRMT1 and PRMT4 are the two major PRMTs responsible for nuclear protein ADMA modification[44]. Therefore, we examined the consequence of RNAi-mediated knockdown of *PRMT1* and *PRMT4* in LRP6(fl/fl);LDLR-/- and SM22-Cre;LRP6(fl/fl);LDLR-/- primary VSM, emphasizing *OPN* expression. Knockdown of *PRMT1* increased *OPN* expression in both genotypes (Figure 6A), indicating a suppressive role. By contrast, knockdown of *PRMT4* reduced *OPN* upregulation in SM22-Cre;LRP6(fl/fl);LDLR-/- cultures -- indicating a sustentacular role (Figure 6B). However, while nuclear protein levels of USF1 increased in SM22-Cre;LRP6(fl/fl);LDLR-/- mice, PRMT4 levels did not (Figure 6C–6D), suggesting that ADMA accumulation might relate to alterations in arginine N-methyl group turnover.

The protein arginine demethylase Jmjd6 inhibits osteochondrogenic gene expression in VSM and USF1-dependent transactivation

Because nuclear ADMA accumulation was altered in the absence of increased nuclear PRMT4, we examined the expression of *Jmjd6*[45, 46] and *PADI4*[47], genes encoding broad spectrum nuclear arginine demethylase and deiminase activities, respectively, that remove the arginine N-methyl signature. As shown in Figure 7A, the levels of both *Jmjd6* and *PADI4* mRNAs were reduced in SM22-Cre;LRP6(fl/fl);LDLR-/- mice, with concomitant upregulation of *OPN* and nuclear ADMA protein accumulation. However, only siRNA targeting *Jmjd6* increased *OPN* and *TNAP* gene expression in control VSM cultures (Figure 7B; Figure XXIII); *PADI4* siRNA reduced mRNA accumulation for select osteochondrogenic genes (Figure 7C). Moreover, Jmjd6 expression inhibited USF1 activation of the OPN promoter (Figure (7D) while PADI4 did not (Figure XXIV).

In HEK cells, USF1 is not ADMA modified, but a low-molecular weight ADMA protein co-immunoprecipitated with FLAG-tagged USF1 (supplement Figure XXV). The size of this ADMA protein, 17 kDa, suggested it might be histone H3. Western blot analysis confirmed H3 co-precipitation with USF1, revealed the presence of the PRMT4-specific H3R17Me2a signature[48], and demonstrated USF1-associated H3R17Me2a was reduced by co-expression of Jmjd6 (Figure 7E and 7F). Furthermore, USF1 immunoprecipitates from LRP6-deficient VSM cultures contain increased histone H3 with the H3R17Me2a signature (Figure 7G). Thus, Jmjd6 inhibits the osteochondrogenic phenotype in VSM, antagonizes USF1-dependent transcriptional activation of *OPN* gene expression, and reduces PRMT4-dependent histone signatures in USF1 protein complexes.

ML141 inhibits USF1 protein accumulation, osteochondrogenic gene expression, TNAP upregulation and calcification in VSM cultures from SM22-Cre;LRP6(fl/fl);LDLR-/- mice

ML141 treatment down-regulated a subset of nuclear ADMA proteins upregulated with LRP6 deficiency (Figure XXVI) -- and reversed the nuclear USF1 protein accumulation and OPN chromatin association arising in SM22-Cre;LRP6(fl/fl);LDLR-/- VSM (Figure 8A; Figure XXVII-XXVIII). Since ML141 inhibited Fzd10 activation of noncanonical Wnt signaling and USF1-dependent *OPN* expression (vide supra), we assessed the impact of ML141 on osteochondrogenic programs upregulated by LRP6 deficiency. Like *OPN, TNAP* and *Col10A1* were reduced by ML141 (Figure 8B and 8C). Interestingly, Wnt ligand genes including *Wnt4*, *Wnt5a*, and *Wnt5b* were concomitantly down-regulated by ML141 in LRP6-deficient VSM while *Jmjd6* was unaffected (Figure XXIX). TNAP enzyme activity – necessary for OPN dephosphorylation and osteochondrogenic mineralization[29] -- was upregulated in SM22-Cre;LRP6(fl/fl);LDLR-/- VSM and inhibited by ML141 treatment (Figure 8D). Consistent with this, calcium deposition quantified by Alizarin red staining was significantly increased in SM22-Cre;LRP6(fl/fl);LDLR-/- VSM and inhibited by ML141 treatment (Figure 8E, 8F). Thus LRP6 restrains vascular noncanonical Wnt signals sensitive to ML141 that promote osteochondrogenic responses, mediated in part via USF1- and arginine methylation – dependent relays (Figure 8G).

DISCUSSION

There are three principal findings of this study that help advance our understanding of arteriosclerotic calcification. Firstly, LRP6 signaling plays a cell-autonomous role in regulating the osteochondrogenic response within the VSM lineage. The VSM functions of LRP6 in arteriosclerotic calcification have not been previously characterized. Surprisingly, in addition to conveying canonical signals, LRP6 restrains noncanonical signals that reinforce osteochondrogenic trans-differentiation and mineralization of VSM[49]. Based upon lineage tracing, Speer estimated that approximately 80% of mineralizing cells in the vessel wall arise from this process; the remaining 20% reflect lineage allocation of regional or circulating osteoprogenitors[49]. Elegant studies by Mani first identified the private mutation LRP6(R611C) as causing a precocious atherosclerosis-osteoporosis syndrome[18, 22], and hypomorphic function may also extend to reduced inhibition of noncanonical signals[18]. Secondly, USF1 emerges as a novel mediator of noncanonical Wnt signaling alongside the Jun/ATF and Ca++/NFAT pathways. The role of USF1 as relevant to the β-globin locus control region[50], glucose signaling[41], and lipid homeostasis[51] is well appreciated, and the genetic link between USF1 and combined hyperlipidemia has been established in parallel with the identification of USF1 within atherosclerotic plaques [51]. As in bone and cartilage[29, 36], cdc42-modulated NFAT signaling will also be an important component of the VSM osteochondrogenic response during arteriosclerotic calcification along with Runx2 and USF1. Given that ML141 inhibits VSM biomineralization – and cdc42's role in vascular inflammation[52] and endochondral ossification[53] -- we speculate that modulators of the cdc42/Rac1 family may prove useful in treating arteriosclerosis. Thirdly, discovery that LRP6 functionally and physically interacts with the protein arginine methylation cascade reveals a new dimension in LRP biology. Our data indicate that non-nuclear PRMT1 associated with LRP6 is part of a pathway suppressing noncanonical signals, while nuclear

PRMT4 supports the osteochondrogenic phenotype in collaboration with osteogenic transcription factors[29]. Others have noted that nuclear PRMT4 (CARM1) forms a complex with Jmjd6[45]. Whether nuclear vs. non-nuclear pools of PRMT1 differentially impact LRP6 signaling remains to be studied.

PRMT4 plays an important role in endochondral bone formation[54] and regulation of estrogen receptor methylation[45] in concert with Jmjd6. Since USF1 lacks overt ADMA modification, we anticipate that proteinaceous partners of USF1 will be directed for ADMA modification. Our data indicate that histone H3 – bearing the H3R17Me2a signature of PRMT4 – is one component of the protein complexes associated with USF1. It remains to be determined whether affinity of USF1 for chromatin is enhanced by H3R17Me2a. USF1 dimerizes with other bHLH and leucine zipper transcription factors to create unique DNA binding specificities[55]. Furthermore, USF1 recruits nuclear PRMT1 to the β-globin locus control region to preserve euchromatin structure via H4R3Me2a formation[50]. It will be important to elucidate the USF1 interactome and its regulation by noncanonical signals.

Fzd9 and Fzd10 are closely related family members that convey noncanonical Wnt signals[31, 35]. Upregulation of noncanonical Fzd10 signaling participates in the pathobiology of synovial sarcoma[35]. Conversely, Fzd9-null mice exhibit reduced endochondral bone formation during fracture repair, arising from deficiency in noncanonical signals necessary for osteoblast maturation and mineralization[31]. It remains to be determined the relative extent to which canonical vs. noncanonical Wnt signals contribute to arterial calcification in the LDLR-/- model. As noted, osteogenic lineage allocation is promoted by *Msx* and canonical *Wnt* signals[5, 29] -- but these signals need to be down-regulated to permit osteoblast maturation[29]. This sequence is emerging as important for the osteogenic programming of vascular progenitors[9, 49]. VSM trans-differentiation is responsible for a majority of the vascular osteochondrogenic cell “load”[49]. We propose that upregulation of noncanonical Fzd activity with LRP6 deficiency enhances VSM osteochondrogenic trans-differentiation in response to metabolic stress.

Our study has limitations. The composition of the LRP6 complex that negatively regulates noncanonical Fzd relays remains to be determined. It’s interesting to note that PRMT1 modifies G3BP family members[56]. Because G3BP1 localizes GTPase activating complexes[56], homologs might be involved in negative regulation of cdc42. However, VSM LRP6 likely orchestrates protein-protein interactions between multiple regulatory components of the noncanonical pathway[15]. Furthermore, LRP6 forms heterodimers with LRP5 [57, 57] Given that LRP5 activity drives pro-sclerotic canonical Wnt signaling in valve calcification[16], it remains probable that heterodimeric interactions between specific LRPs and Fzds finely tune signaling via the canonical and noncanonical pathways. LRP5/6 heterodimers confer selectivity for Wnt ligand activation[57]; this combinatorial complexity indicates that changes in levels of a specific LRP receptor will impact canonical signaling as a function of the prevailing Wnt ligand milieu while directly modulating noncanonical tone. Even though we targeted LRP6 expression in the VSM lineage, secondary alterations in the monocyte/macrophage lineage may contribute to arteriosclerosis[58]. Innovative studies very recently published have identified that a subset of inflammatory mural macrophages arise from the VSM lineage (reviewed in refs.[59, 60]). Future studies will assess whether VSM

LRP6 orchestrates phenotypic modulation and myeloid cell differentiation, recruitment and function in vascular lesions in response to metabolic stressors. As in bone[31] stage-specific roles for canonical and noncanonical Wnts are emerging in the regulatory sequence that drives arterial osteochondrogenic programming. The evolving models of LRP-dependent vascular disease have yet to fully address this sequence. *In vivo* quantitative measures of ligand expression and signal activation are needed to temporally and spatially resolve the contributions of specific Wnt ligand-receptor engagement to disease biology. Finally, Runx2 -- the master osteochondrogenic transcriptional regulator [29] -- is post-transcriptionally activated in VSM[61]. How USF1 supports programs enabled by Runx2 remains to be determined. USF1 increases with osteoblast differentiation[62], and USF mechanisms encompass the maintenance of chromatin structure necessary for tissue-specific enhancer function[50]. Nevertheless, the discovery that ML141 down-regulates noncanonical sclerotic programs restrained by LRP6 signaling indicates that strategies targeting the cdc42-related GTPases can function as LRP6 mimetics -- and might mitigate vascular disease in patients afflicted with diabetes and dyslipidemia.

Supplementary Material

Refer to Web version on PubMed Central for supplementary material.

Acknowledgments

SOURCES OF FUNDING

Supported by NIH grants HL081138, HL069229, and HL114806 to D.A.T. and AR053292 to B.O.W.

Nonstandard Abbreviations and Acronyms

ADMA	asymmetric dimethylarginine
bHLH-zip	basic helix-loop-helix – leucine zipper transcription factor
BMC/BMD	bone mineral content/bone mineral density
BMP	bone morphogenetic protein
BrdU	bromodeoxyuridine
CARM1	coactivator-associated arginine methyltransferase 1, a.k.a. PRMT4
Cdc42	cell division cycle 42, a Rac1 family member GTPase
ChIP	chromatin immunoprecipitation
CMV	cytomegalovirus promoter/enhancer vector
Col10A1	type X collagen gene alpha 1 chain
DAPI	4′,6-diamidino-2-phenylindole
DXA	dual electron X-ray absorptiometry
eIF	eukaryotic translation initiation factor
FLAG	amino acid epitope D-Y-K-D-D-D-D-K

FLAG-IP	immunoprecipation with anti-FLAG epitope antibody
Fzd	frizzled Wnt GPCR receptor
G3BP	Ras-GAP SH3 domain binding protein
GAP	GTPase activating protein
H3R17Me2a	histone H3 asymmetrically dimethylated on Arg-17, a PRMT4 product
H4R3Me2a	histone H4 asymmetrically dimethylated on Arg-3, a PRMT1 product
HEK	human embryonic kidney cell line
HFD	high fat diet, Harland TD88137 Western diet
Jmjd6	Jumonji domain containing 6 arginine demethylase
Klf5	krüppel like factor 5
LDLR	low density lipoprotein receptor
LEF	lymphoid enhancing factor
LRP	LDL-receptor related protein
LRP6(fl/fl)	LRP6 gene floxed, e.g. flanked by lox P
LRP6-VKO	LRP6 VSM conditional knockout
LUC	luciferase reporter
ML141	cdc42/Rac1 inhibitor, Chemical Abstracts Registry CAS # 71203-35-5
MMP	matrix metalloproteinase
Msx	muscle segment homeobox homolog
Myh11	smooth muscle specific myosin heavy chain 11
NFAT	nuclear factor of activated T cells
OCN	osteocalcin
OPN	osteopontin
Osx	osterix Sp7 transcription factor
PADI	peptidyl arginine deiminase
PRMT	protein arginine N-methyltransferase
RNAi	RNA interference
Runx	Runt-related transcription factor
Sca1	stem cell antigen 1
siRNA	small interfering RNA
SM22-Cre	transgene expressing bacterial Cre recombinase from transgelin promoter
TCF	T cell factor

TK	HSV Thymidine kinase promoter
TNAP	bone alkaline phosphatase, tissue non-specific alkaline phosphatase, akp2
TNF	tumor necrosis factor
USF	upstream stimulatory factor
VSM	vascular smooth muscle lineage
Wnt	Wingless/int-1 family member

References

1. Thompson B, Towler DA. Arterial calcification and bone physiology: Role of the bone-vascular axis. Nature reviews Endocrinology. 2012; 8:529–543.
2. Demer LL, Tintut Y. Inflammatory, metabolic, and genetic mechanisms of vascular calcification. Arteriosclerosis, thrombosis, and vascular biology. 2014; 34:715–723.
3. Bostrom KI, Jumabay M, Matveyenko A, Nicholas SB, Yao Y. Activation of vascular bone morphogenetic protein signaling in diabetes mellitus. Circulation research. 2011; 108:446–457. [PubMed: 21193740]
4. Woldt E, Terrand J, Mlih M, Matz RL, Bruban V, Coudane F, Foppolo S, El Asmar Z, Chollet ME, Ninio E, Bednarczyk A, Thierse D, Schaeffer C, Van Dorsselaer A, Boudier C, Wahli W, Chambon P, Metzger D, Herz J, Boucher P. The nuclear hormone receptor ppargamma counteracts vascular calcification by inhibiting wnt5a signalling in vascular smooth muscle cells. Nature communications. 2012; 3:1077.
5. Shao JS, Cheng SL, Pingsterhaus JM, Charlton-Kachigian N, Loewy AP, Towler DA. Msx2 promotes cardiovascular calcification by activating paracrine wnt signals. The Journal of clinical investigation. 2005; 115:1210–1220. [PubMed: 15841209]
6. Beazley KE, Nurminsky D, Lima F, Gandhi C, Nurminskaya MV. Wnt16 attenuates tgfbeta-induced chondrogenic transformation in vascular smooth muscle. Arteriosclerosis, thrombosis, and vascular biology. 2015
7. Derwall M, Malhotra R, Lai CS, Beppu Y, Aikawa E, Seehra JS, Zapol WM, Bloch KD, Yu PB. Inhibition of bone morphogenetic protein signaling reduces vascular calcification and atherosclerosis. Arteriosclerosis, thrombosis, and vascular biology. 2012; 32:613–622.
8. Schreyer SA, Vick C, Lystig TC, Mystkowski P, LeBoeuf RC. Ldl receptor but not apolipoprotein e deficiency increases diet-induced obesity and diabetes in mice. American journal of physiology Endocrinology and metabolism. 2002; 282:E207–214. [PubMed: 11739102]
9. Cheng SL, Behrmann A, Shao JS, Ramachandran B, Krchma K, Bello Arredondo Y, Kovacs A, Mead M, Maxson R, Towler DA. Targeted reduction of vascular msx1 and msx2 mitigates arteriosclerotic calcification and aortic stiffness in ldlr-deficient mice fed diabetogenic diets. Diabetes. 2014; 63:4326–4337. [PubMed: 25056439]
10. Cheng SL, Shao JS, Behrmann A, Krchma K, Towler DA. Dkk1 and msx2-wnt7b signaling reciprocally regulate the endothelial-mesenchymal transition in aortic endothelial cells. Arteriosclerosis, thrombosis, and vascular biology. 2013; 33:1679–1689.
11. Tu X, Joeng KS, Nakayama KI, Nakayama K, Rajagopal J, Carroll TJ, McMahon AP, Long F. Noncanonical wnt signaling through g protein-linked pkcdelta activation promotes bone formation. Developmental cell. 2007; 12:113–127. [PubMed: 17199045]
12. Joiner DM, Ke J, Zhong Z, Xu HE, Williams BO. Lrp5 and lrp6 in development and disease. Trends in endocrinology and metabolism: TEM. 2013; 24:31–39. [PubMed: 23245947]
13. Rao TP, Kuhl M. An updated overview on wnt signaling pathways: A prelude for more. Circulation research. 2010; 106:1798–1806. [PubMed: 20576942]

14. Esen E, Chen J, Karner CM, Okunade AL, Patterson BW, Long F. Wnt-lrp5 signaling induces warburg effect through mtorc2 activation during osteoblast differentiation. Cell Metab. 2013; 17:745–755. [PubMed: 23623748]
15. Grumolato L, Liu G, Mong P, Mudbhary R, Biswas R, Arroyave R, Vijayakumar S, Economides AN, Aaronson SA. Canonical and noncanonical wnts use a common mechanism to activate completely unrelated coreceptors. Genes & development. 2010; 24:2517–2530. [PubMed: 21078818]
16. Rajamannan NM. The role of lrp5/6 in cardiac valve disease: Experimental hypercholesterolemia in the apoe-/-/lrp5-/- mice. Journal of cellular biochemistry. 2011; 112:2987–2991. [PubMed: 21678468]
17. Joeng KS, Schumacher CA, Zylstra-Diegel CR, Long F, Williams BO. Lrp5 and lrp6 redundantly control skeletal development in the mouse embryo. Developmental biology. 2011; 359:222–229. [PubMed: 21924256]
18. Mani A, Radhakrishnan J, Wang H, Mani A, Mani MA, Nelson-Williams C, Carew KS, Mane S, Najmabadi H, Wu D, Lifton RP. Lrp6 mutation in a family with early coronary disease and metabolic risk factors. Science. 2007; 315:1278–1282. [PubMed: 17332414]
19. Demer L, Tintut Y. The bone-vascular axis in chronic kidney disease. Current opinion in nephrology and hypertension. 2010; 19:349–353. [PubMed: 20508522]
20. Holtwick R, Gotthardt M, Skryabin B, Steinmetz M, Potthast R, Zetsche B, Hammer RE, Herz J, Kuhn M. Smooth muscle-selective deletion of guanylyl cyclase-a prevents the acute but not chronic effects of anp on blood pressure. Proceedings of the National Academy of Sciences of the United States of America. 2002; 99:7142–7147. [PubMed: 11997476]
21. Zhong Z, Baker JJ, Zylstra-Diegel CR, Williams BO. Lrp5 and lrp6 play compensatory roles in mouse intestinal development. Journal of cellular biochemistry. 2012; 113:31–38. [PubMed: 21866564]
22. Go GW, Srivastava R, Hernandez-Ono A, Gang G, Smith SB, Booth CJ, Ginsberg HN, Mani A. The combined hyperlipidemia caused by impaired wnt-lrp6 signaling is reversed by wnt3a rescue. Cell Metab. 2014; 19:209–220. [PubMed: 24506864]
23. Cheng SL, Shao JS, Halstead LR, Distelhorst K, Sierra O, Towler DA. Activation of vascular smooth muscle parathyroid hormone receptor inhibits wnt/beta-catenin signaling and aortic fibrosis in diabetic arteriosclerosis. Circulation research. 2010; 107:271–282. [PubMed: 20489161]
24. Jho EH, Zhang T, Domon C, Joo CK, Freund JN, Costantini F. Wnt/beta-catenin/tcf signaling induces the transcription of axin2, a negative regulator of the signaling pathway. Molecular and cellular biology. 2002; 22:1172–1183. [PubMed: 11809808]
25. Ziemer LT, Pennica D, Levine AJ. Identification of a mouse homolog of the human bteb2 transcription factor as a beta-catenin-independent wnt-1-responsive gene. Molecular and cellular biology. 2001; 21:562–574. [PubMed: 11134343]
26. Laudes M, Oberhauser F, Schulte DM, Freude S, Bilkovski R, Mauer J, Rappl G, Abken H, Hahn M, Schulz O, Krone W. Visfatin/pbef/nampt and resistin expressions in circulating blood monocytes are differentially related to obesity and type 2 diabetes in humans. Hormone and metabolic research = Hormon- und Stoffwechselforschung = Hormones et metabolisme. 2010; 42:268–273. [PubMed: 20091460]
27. Mayr M, Zampetaki A, Sidibe A, Mayr U, Yin X, De Souza AI, Chung YL, Madhu B, Quax PH, Hu Y, Griffiths JR, Xu Q. Proteomic and metabolomic analysis of smooth muscle cells derived from the arterial media and adventitial progenitors of apolipoprotein e-deficient mice. Circulation research. 2008; 102:1046–1056. [PubMed: 18388323]
28. Wolak T. Osteopontin - a multi-modal marker and mediator in atherosclerotic vascular disease. Atherosclerosis. 2014; 236:327–337. [PubMed: 25128758]
29. Cohen MM Jr. The new bone biology: Pathologic, molecular, and clinical correlates. American journal of medical genetics Part A. 2006; 140:2646–2706. [PubMed: 17103447]
30. Kubota T, Michigami T, Sakaguchi N, Kokubu C, Suzuki A, Namba N, Sakai N, Nakajima S, Imai K, Ozono K. Lrp6 hypomorphic mutation affects bone mass through bone resorption in mice and

impairs interaction with mesd. Journal of bone and mineral research : the official journal of the American Society for Bone and Mineral Research. 2008; 23:1661–1671.

31. Heilmann A, Schinke T, Bindl R, Wehner T, Rapp A, Haffner-Luntzer M, Nemitz C, Liedert A, Amling M, Ignatius A. The wnt serpentine receptor frizzled-9 regulates new bone formation in fracture healing. PloS one. 2013; 8:e84232. [PubMed: 24391920]
32. Okamoto M, Udagawa N, Uehara S, Maeda K, Yamashita T, Nakamichi Y, Kato H, Saito N, Minami Y, Takahashi N, Kobayashi Y. Noncanonical wnt5a enhances wnt/beta-catenin signaling during osteoblastogenesis. Scientific reports. 2014; 4:4493. [PubMed: 24670389]
33. Chang J, Sonoyama W, Wang Z, Jin Q, Zhang C, Krebsbach PH, Giannobile W, Shi S, Wang CY. Noncanonical wnt-4 signaling enhances bone regeneration of mesenchymal stem cells in craniofacial defects through activation of p38 mapk. The Journal of biological chemistry. 2007; 282:30938–30948. [PubMed: 17720811]
34. Lyons JP, Mueller UW, Ji H, Everett C, Fang X, Hsieh JC, Barth AM, McCrea PD. Wnt-4 activates the canonical beta-catenin-mediated wnt pathway and binds frizzled-6 crd: Functional implications of wnt/beta-catenin activity in kidney epithelial cells. Experimental cell research. 2004; 298:369–387. [PubMed: 15265686]
35. Fukukawa C, Nagayama S, Tsunoda T, Toguchida J, Nakamura Y, Katagiri T. Activation of the non-canonical dvl-rac1-jnk pathway by frizzled homologue 10 in human synovial sarcoma. Oncogene. 2009; 28:1110–1120. [PubMed: 19137009]
36. Bradley EW, Drissi MH. Wnt5a regulates chondrocyte differentiation through differential use of the can/nfat and ikk/nf-kappab pathways. Molecular endocrinology. 2010; 24:1581–1593. [PubMed: 20573686]
37. Ring L, Perobner I, Karow M, Jochum M, Neth P, Faussner A. Reporter gene hek 293 cells and wnt/frizzled fusion proteins as tools to study wnt signaling pathways. Biological chemistry. 2011; 392:1011–1020. [PubMed: 21864196]
38. Surviladze, Z.; Waller, A.; Strouse, JJ.; Bologa, C.; Ursu, O.; Salas, V.; Parkinson, JF.; Phillips, GK.; Romero, E.; Wandinger-Ness, A.; Sklar, LA.; Schroeder, C.; Simpson, D.; Noth, J.; Wang, J.; Golden, J.; Aube, J. Probe reports from the nih molecular libraries program. Bethesda (MD): 2010. A potent and selective inhibitor of cdc42 gtpase.
39. Yuan K, Orcholski ME, Panaroni C, Shuffle EM, Huang NF, Jiang X, Tian W, Vladar EK, Wang L, Nicolls MR, Wu JY, de Jesus Perez VA. Activation of the wnt/planar cell polarity pathway is required for pericyte recruitment during pulmonary angiogenesis. The American journal of pathology. 2015; 185:69–84. [PubMed: 25447046]
40. Bilkovski R, Schulte DM, Oberhauser F, Gomolka M, Udelhoven M, Hettich MM, Roth B, Heidenreich A, Gutschow C, Krone W, Laudes M. Role of wnt-5a in the determination of human mesenchymal stem cells into preadipocytes. The Journal of biological chemistry. 2010; 285:6170–6178. [PubMed: 20032469]
41. Bidder M, Shao JS, Charlton-Kachigian N, Loewy AP, Semenkovich CF, Towler DA. Osteopontin transcription in aortic vascular smooth muscle cells is controlled by glucose-regulated upstream stimulatory factor and activator protein-1 activities. The Journal of biological chemistry. 2002; 277:44485–44496. [PubMed: 12200434]
42. Shutes A, Onesto C, Picard V, Leblond B, Schweighoffer F, Der CJ. Specificity and mechanism of action of eht 1864, a novel small molecule inhibitor of rac family small gtpases. The Journal of biological chemistry. 2007; 282:35666–35678. [PubMed: 17932039]
43. Goulet I, Gauvin G, Boisvenue S, Cote J. Alternative splicing yields protein arginine methyltransferase 1 isoforms with distinct activity, substrate specificity, and subcellular localization. The Journal of biological chemistry. 2007; 282:33009–33021. [PubMed: 17848568]
44. Bedford MT, Clarke SG. Protein arginine methylation in mammals: Who, what, and why. Molecular cell. 2009; 33:1–13. [PubMed: 19150423]
45. Poulard C, Rambaud J, Hussein N, Corbo L, Le Romancer M. Jmjd6 regulates eralpha methylation on arginine. PloS one. 2014; 9:e87982. [PubMed: 24498420]
46. Chang B, Chen Y, Zhao Y, Bruick RK. Jmjd6 is a histone arginine demethylase. Science. 2007; 318:444–447. [PubMed: 17947579]

47. Kolodziej S, Kuvardina ON, Oellerich T, Herglotz J, Backert I, Kohrs N, Buscato E, Wittmann SK, Salinas-Riester G, Bonig H, Karas M, Serve H, Proschak E, Lausen J. Padi4 acts as a coactivator of tal1 by counteracting repressive histone arginine methylation. Nature communications. 2014; 5:3995.
48. Gayatri S, Bedford MT. Readers of histone methylarginine marks. Biochimica et biophysica acta. 2014; 1839:702–710. [PubMed: 24583552]
49. Naik V, Leaf EM, Hu JH, Yang HY, Nguyen NB, Giachelli CM, Speer MY. Sources of cells that contribute to atherosclerotic intimal calcification: An in vivo genetic fate mapping study. Cardiovascular research. 2012; 94:545–554. [PubMed: 22436847]
50. Huang S, Li X, Yusufzai TM, Qiu Y, Felsenfeld G. Usf1 recruits histone modification complexes and is critical for maintenance of a chromatin barrier. Molecular and cellular biology. 2007; 27:7991–8002. [PubMed: 17846119]
51. Fan YM, Hernesniemi J, Oksala N, Levula M, Raitoharju E, Collings A, Hutri-Kahonen N, Juonala M, Marniemi J, Lyytikainen LP, Seppala I, Mennander A, Tarkka M, Kangas AJ, Soininen P, Salenius JP, Klopp N, Illig T, Laitinen T, Ala-Korpela M, Laaksonen R, Viikari J, Kahonen M, Raitakari OT, Lehtimaki T. Upstream transcription factor 1 (usf1) allelic variants regulate lipoprotein metabolism in women and usf1 expression in atherosclerotic plaque. Scientific reports. 2014; 4:4650. [PubMed: 24722012]
52. Ito TK, Yokoyama M, Yoshida Y, Nojima A, Kassai H, Oishi K, Okada S, Kinoshita D, Kobayashi Y, Fruttiger M, Aiba A, Minamino T. A crucial role for cdc42 in senescence-associated inflammation and atherosclerosis. PloS one. 2014; 9:e102186. [PubMed: 25057989]
53. Suzuki W, Yamada A, Aizawa R, Suzuki D, Kassai H, Harada T, Nakayama M, Nagahama R, Maki K, Takeda S, Yamamoto M, Aiba A, Baba K, Kamijo R. Cdc42 is critical for cartilage development during endochondral ossification. Endocrinology. 2015; 156:314–322. [PubMed: 25343271]
54. Ito T, Yadav N, Lee J, Furumatsu T, Yamashita S, Yoshida K, Taniguchi N, Hashimoto M, Tsuchiya M, Ozaki T, Lotz M, Bedford MT, Asahara H. Arginine methyltransferase carm1/prmt4 regulates endochondral ossification. BMC developmental biology. 2009; 9:47. [PubMed: 19725955]
55. Massari ME, Murre C. Helix-loop-helix proteins: Regulators of transcription in eucaryotic organisms. Molecular and cellular biology. 2000; 20:429–440. [PubMed: 10611221]
56. Bikkavilli RK, Malbon CC. Arginine methylation of g3bp1 in response to wnt3a regulates beta-catenin mrna. Journal of cell science. 2011; 124:2310–2320. [PubMed: 21652632]
57. Goel S, Chin EN, Fakhraldeen SA, Berry SM, Beebe DJ, Alexander CM. Both lrp5 and lrp6 receptors are required to respond to physiological wnt ligands in mammary epithelial cells and fibroblasts. The Journal of biological chemistry. 2012; 287:16454–16466. [PubMed: 22433869]
58. New SE, Goettsch C, Aikawa M, Marchini JF, Shibasaki M, Yabusaki K, Libby P, Shanahan CM, Croce K, Aikawa E. Macrophage-derived matrix vesicles: An alternative novel mechanism for microcalcification in atherosclerotic plaques. Circulation research. 2013; 113:72–77. [PubMed: 23616621]
59. Fisher EA, Miano JM. Don't judge books by their covers: Vascular smooth muscle cells in arterial pathologies. Circulation. 2014; 129:1545–1547. [PubMed: 24733539]
60. Swirski FK, Nahrendorf M. Do vascular smooth muscle cells differentiate to macrophages in atherosclerotic lesions? Circulation research. 2014; 115:605–606. [PubMed: 25214571]
61. Heath JM, Sun Y, Yuan K, Bradley WE, Litovsky S, Dell'Italia LJ, Chatham JC, Wu H, Chen Y. Activation of akt by o-linked n-acetylglucosamine induces vascular calcification in diabetes mellitus. Circulation research. 2014; 114:1094–1102. [PubMed: 24526702]
62. Zhang Y, Hassan MQ, Li ZY, Stein JL, Lian JB, van Wijnen AJ, Stein GS. Intricate gene regulatory networks of helix-loop-helix (hlh) proteins support regulation of bone-tissue related genes during osteoblast differentiation. Journal of cellular biochemistry. 2008; 105:487–496. [PubMed: 18655182]

Novelty and Significance

What Is Known?

- Paracrine Wnt signaling controls bone mineralization, mediated in part by LDL receptor-related protein (LRP) family heterodimers with frizzled (Fzd) co-receptors.
- Rare hypomorphic mutations in human LRP6 canonical signaling proteins cause autosomal dominant osteoporosis and early cardiometabolic disease.
- Multiple Wnt ligands are expressed in vessels undergoing calcification, suggesting that Wnt signaling plays an important role in arteriosclerosis.

What New Information Does This Article Contribute?

- Deletion of vascular smooth muscle lineage (VSM) LRP6 worsens arteriosclerotic disease in a model of diet-induced insulin-resistant diabetes, dyslipidemia, and cardiovascular calcification.
- Loss of VSM LRP6 enhances Wnt ligand expression and osteochondrogenic signaling via noncanonical Fzd co-receptors, mediated in part by USF1 and protein arginine methyltransferase (PRMT) relays.
- Like LRP6, the cdc42/rac1 G-protein antagonist ML141 inhibits noncanonical Wnt signals that drive VSM mineralization, indicating that certain LRP6 mimetics may prove useful in the treatment of arteriosclerotic calcification.

In this study, we demonstrate that the Wnt co-receptor LRP6 plays a rate-limiting role in restraining VSM noncanonical Wnt signals that drive arteriosclerotic calcification and vascular stiffening with insulin-resistant hyperglycemia and hyperlipidemia. Vascular Wnt ligands, Fzd10-dependent noncanonical signals, and osteochondrogenic mineralization programs are upregulated with reduction in VSM LRP6. We show that PRMTs and the Jmjd6 demethylase are novel components of LRP6-regulated relays that control VSM drift to the osteochondrogenic phenotype. The transcription factor USF1 is identified as a new component of the VSM noncanonical response, regulated at the level of nuclear chromatin complex formation by LRP6, ML141, and Jmjd6. These results reveal novel dimensions of LRP6 vascular biology that provide insights useful for crafting new approaches to treat arteriosclerotic disease.

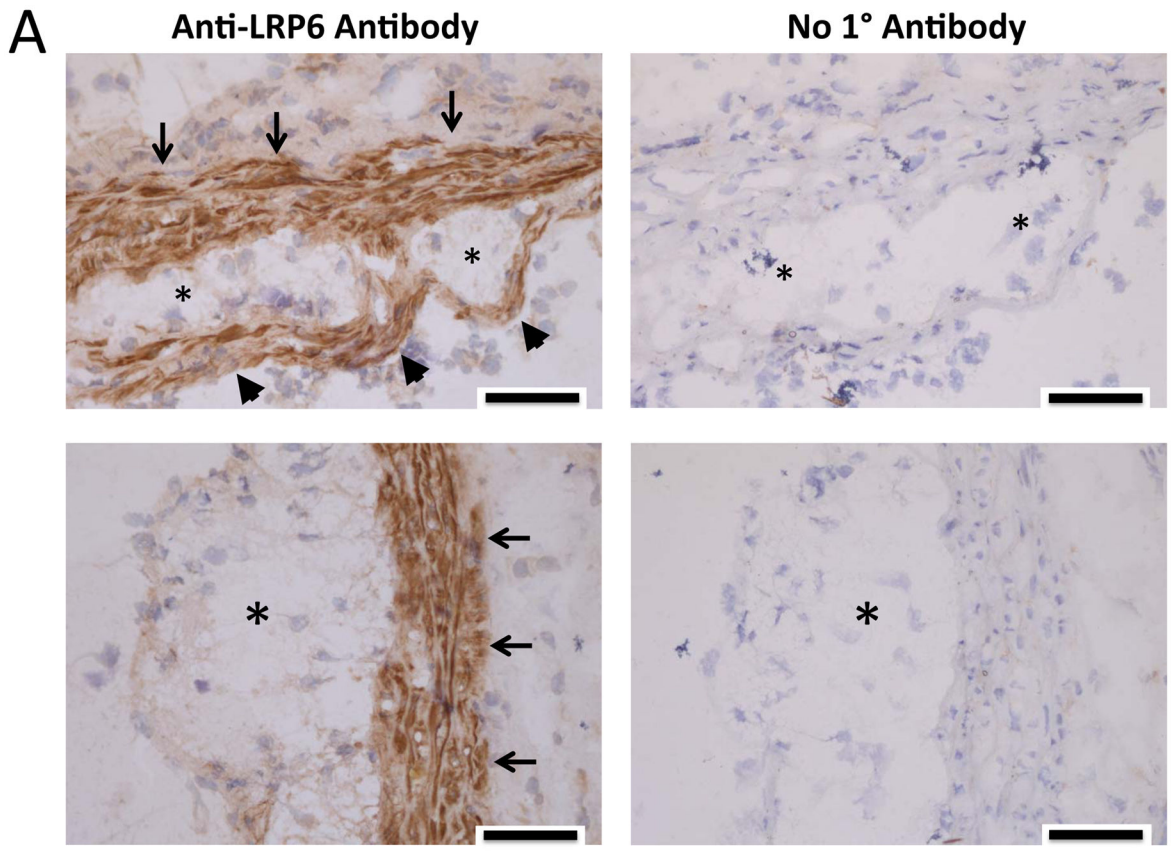

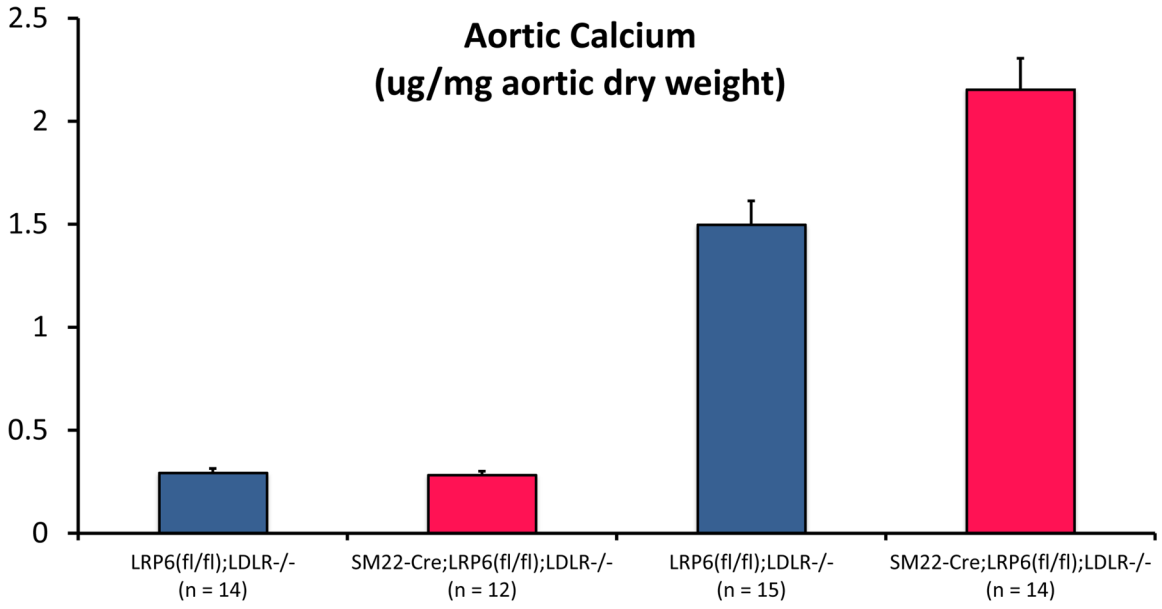

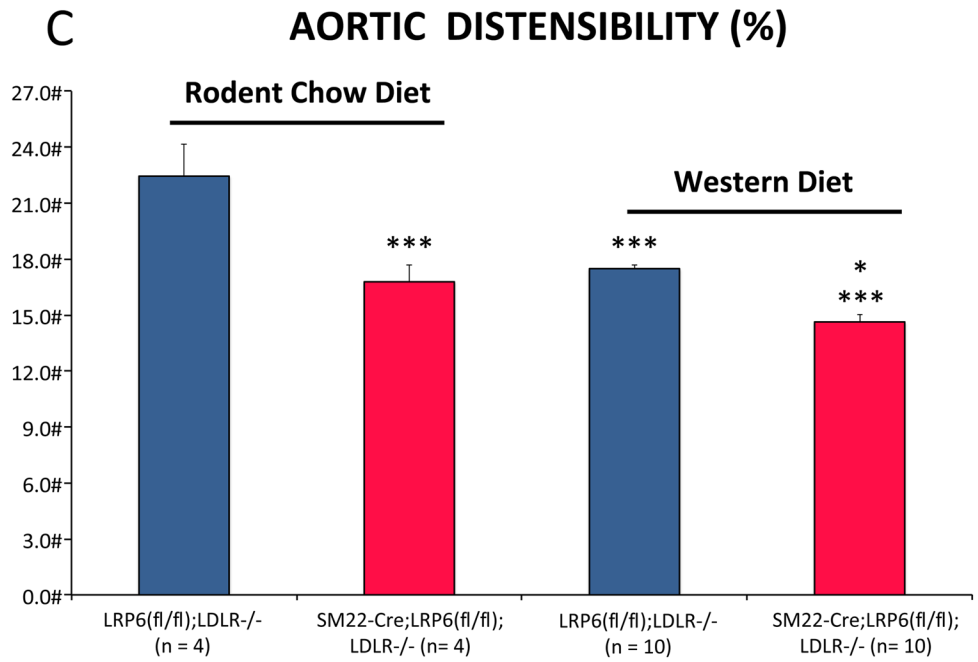

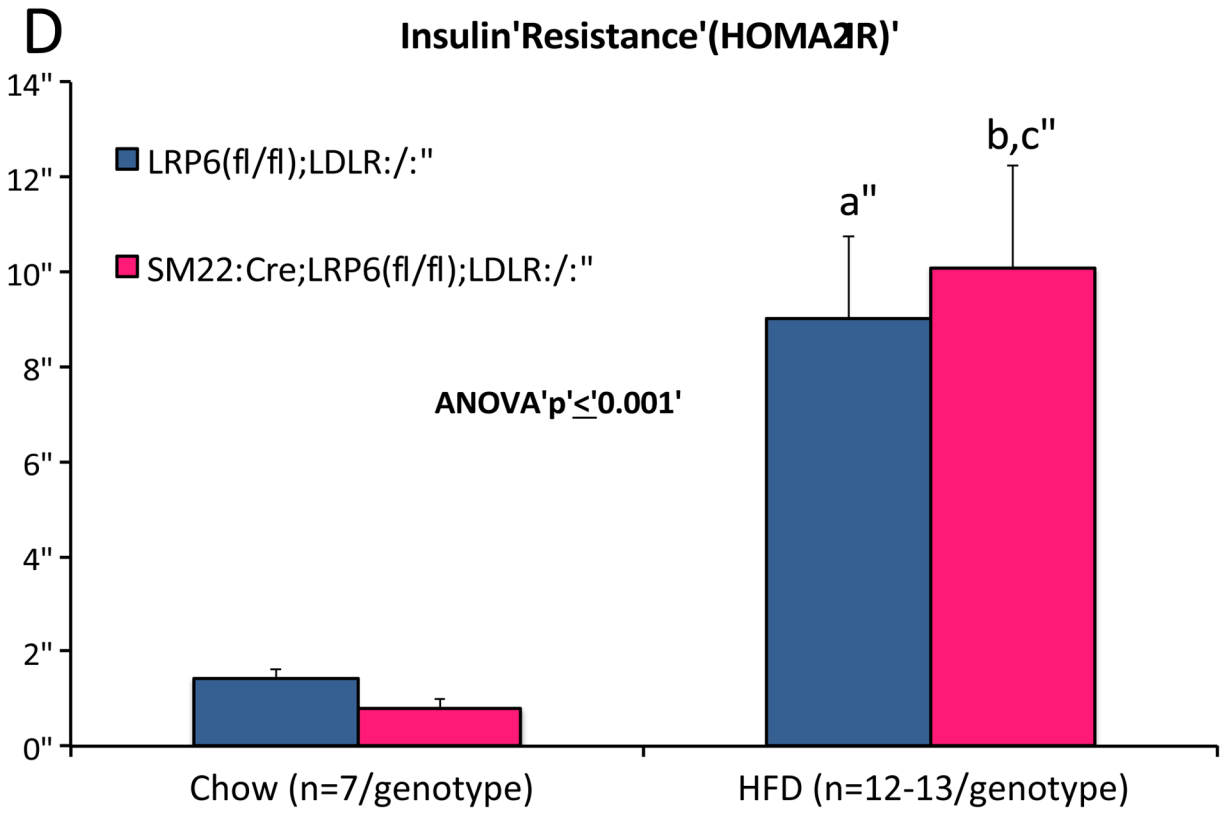

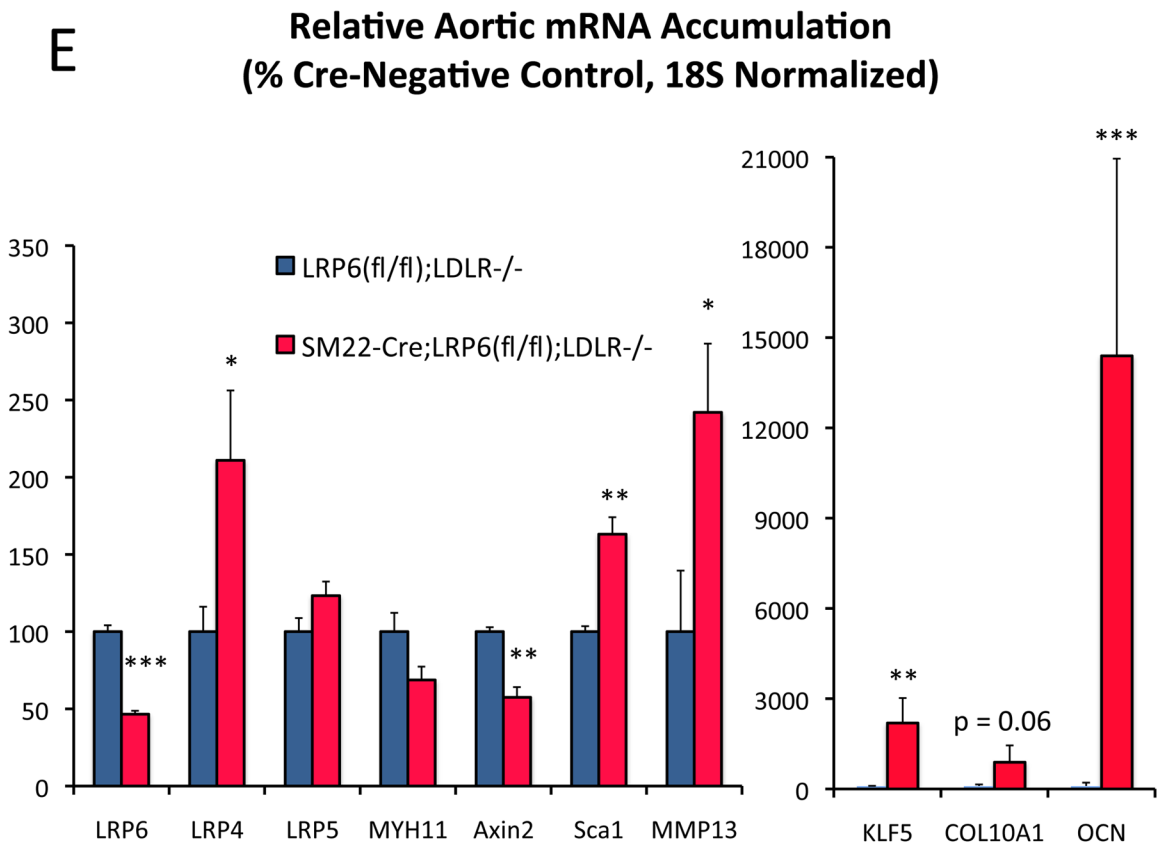

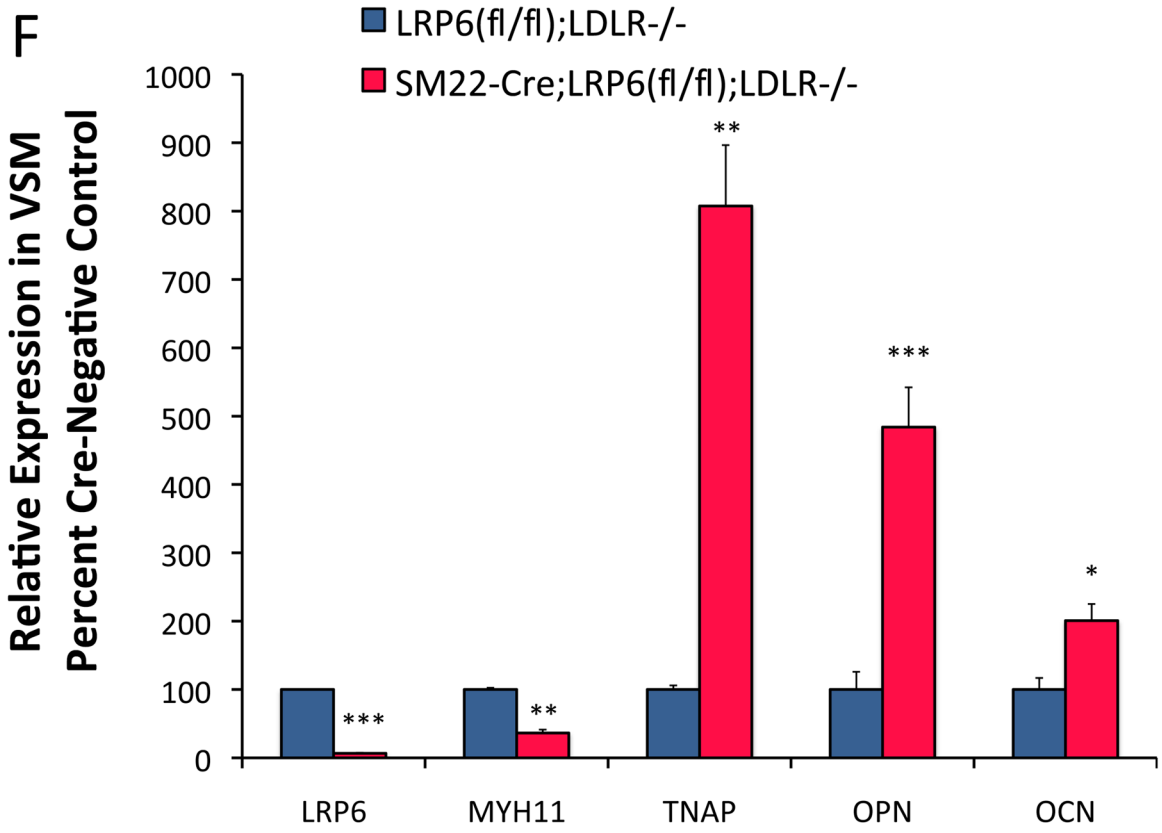

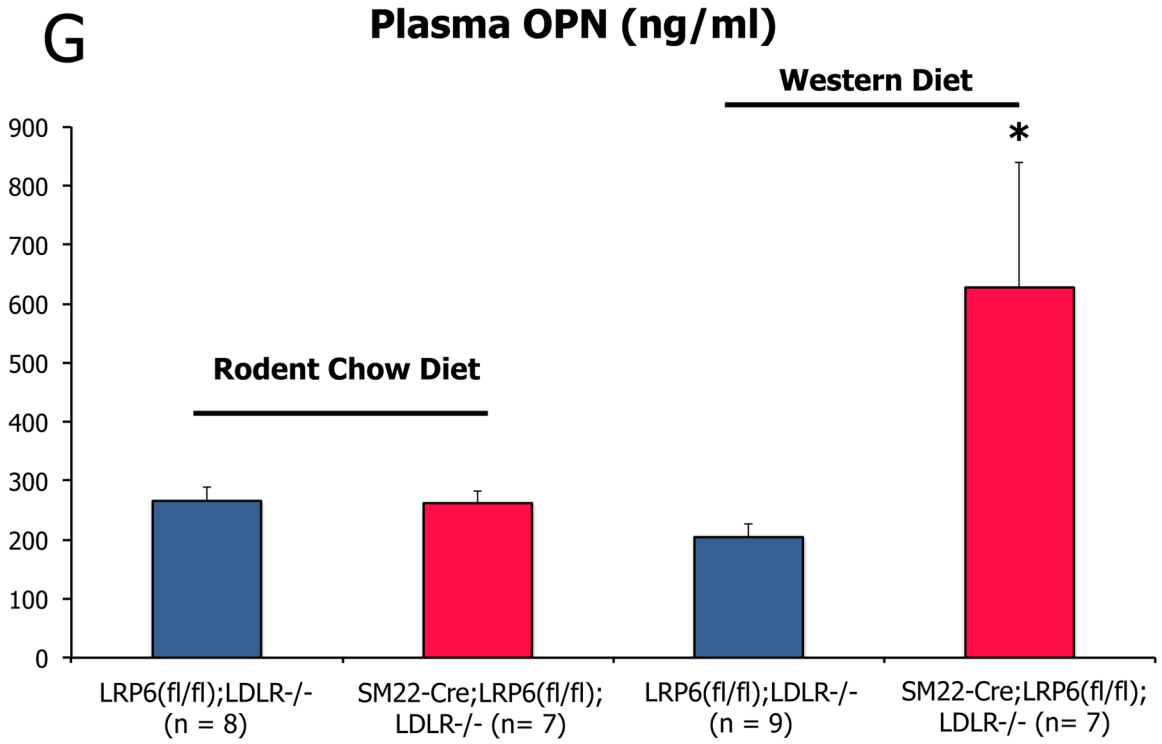

Figure 1. Conditional deletion of LRP6 in VSM increases osteochondrogenic calcification and arterial stiffening in LDLR-/- mice fed high fat diabetogenic diets

Panel A, immunohistochemistry reveals expression of LRP6 in VSM of aortic tunica media (arrows) and atherosclerotic caps (arrowheads) of the aortic sinus. Asterisks overlay atheroma. Scale bar = 50 microns. Coronary artery VSM also expresses LRP6 (Figure S1–S2). Panel B, on HFD aortic calcium content is increased in aortas of SM22-Cre;LRP6(fl/fl);LDLR-/- mice as compared to LRP6(fl/fl);LDLR-/- on HFD or chow-fed controls (11–15 weeks of age). All HFD animals were 17–20 weeks of age at aortic analysis. Numbers of animals in each group were between 12–14 as indicated. ANOVA $p < 0.0001$. a, $p< 0.001$ vs. chow-fed controls; b, $p < 0.01$ vs. Cre-negative mice on HFD by Holm-Sidak's post-hoc testing corrected for multiple comparisons. Panel C, Doppler echocardiography reveals increased vascular stiffness in SM22-Cre;LRP6(fl/fl);LDLR-/- mice, reflected in reduced distensibility (% change in aortic arch diameter from diastole to systole). ANOVA $p < 0.0001$. ***, $p < 0.001$ vs LRP6(fl/fl);LDLR-/- on chow diet*, $p < 0.05$ vs. Cre-minus on Western Diet on post-hoc testing corrected for multiple comparisons. N = 4 to 10 per group as indicated in the X-axis labels. Panel D, HFD-induced insulin resistance did not differ between genotypes. One way ANOVA $p <0.001$; significant differences between the groups as indicated by Holm-Sidak post-hoc test (see also supplement Figures XXII–XXIII). a, $p < 0.05$ vs. chow fed of either genotype; b, $p < 0.05$ vs. chow fed Cre-negative animals; c, $p < 0.01$ between chow fed SM22-Cre;LRP6(fl/fl);LDLR-/- animals. No other differences were significant. Panel E, the aortic expression of osteochondrogenic genes is concomitantly upregulated with reductions in VSM LRP6 expression. *, $p < 0.05$ vs. LRP6(fl/fl);LDLR-/- control; **, $p < 0.01$ vs. control; ***, $p < 0.001$ vs. control by Student's 2-tailed t-test; used throughout unless otherwise indicated. Panel F, cultures of primary aortic VSM also exhibit enhanced osteochondrogenic gene expression in the setting of LRP6 deficiency. *, $p < 0.05$ vs. LRP6(fl/fl);LDLR-/- control; **, $p < 0.01$ vs. control; ***, $p < 0.001$ vs. control by Student's 2-tail t-test; used throughout unless otherwise indicated. Panel G, circulating OPN levels are increased in diabetic SM22-Cre;LRP6(fl/fl);LDLR-/- mice as compared to LRP6(fl/fl);LDLR-/- controls. N = 8, 7, 9, and 7, respectively as indicated. ANOVA $p = 0.022$. * $p < 0.05$ vs. all others by Fisher's LSD post-hoc test, and $p < 0.05$ vs. Cre-minus control on HFD after correction for multiple comparisons.

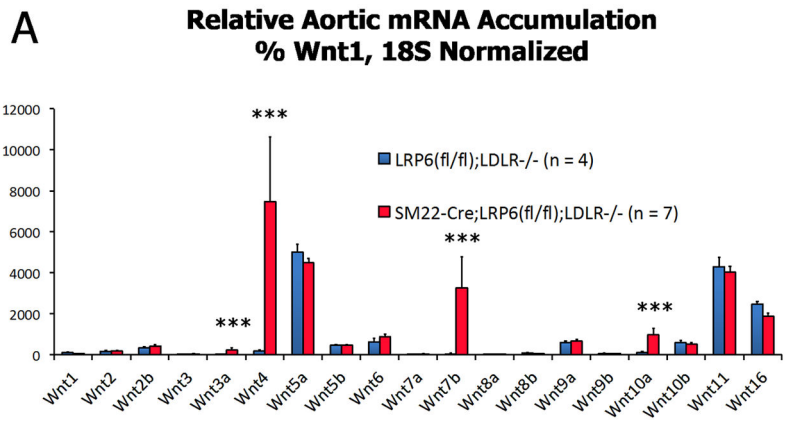

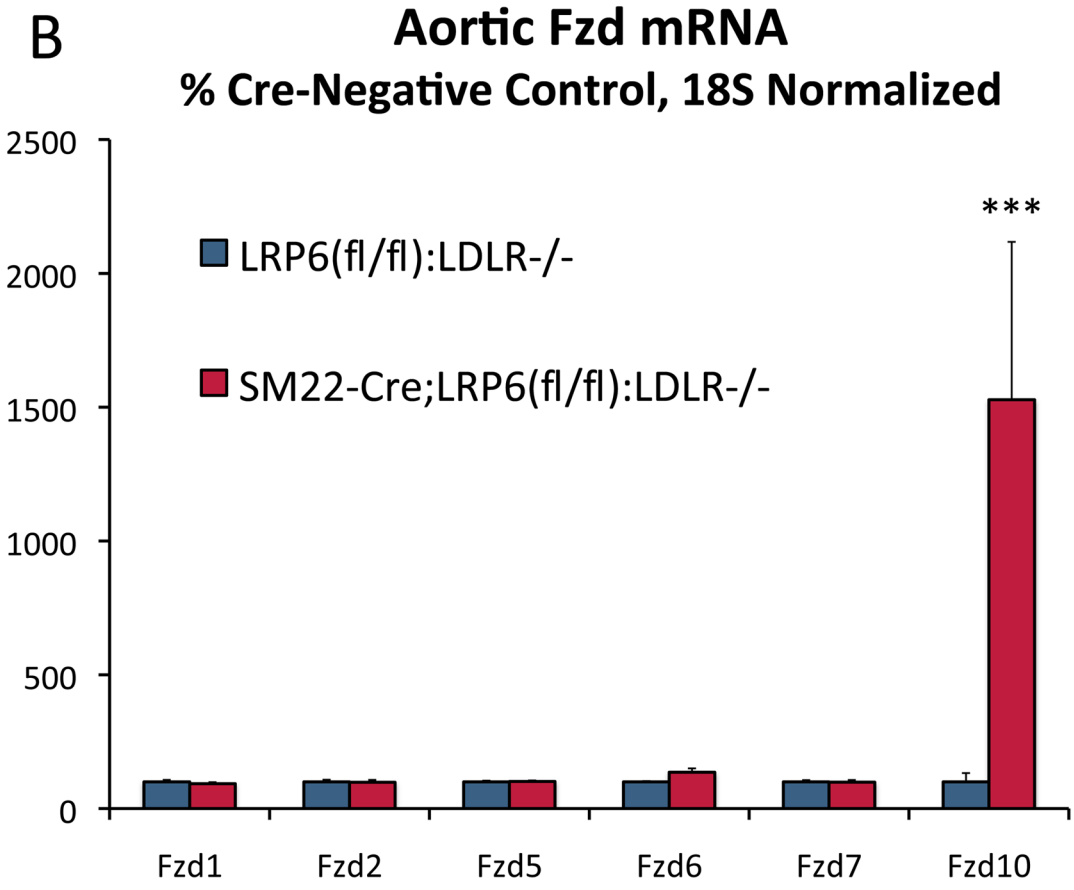

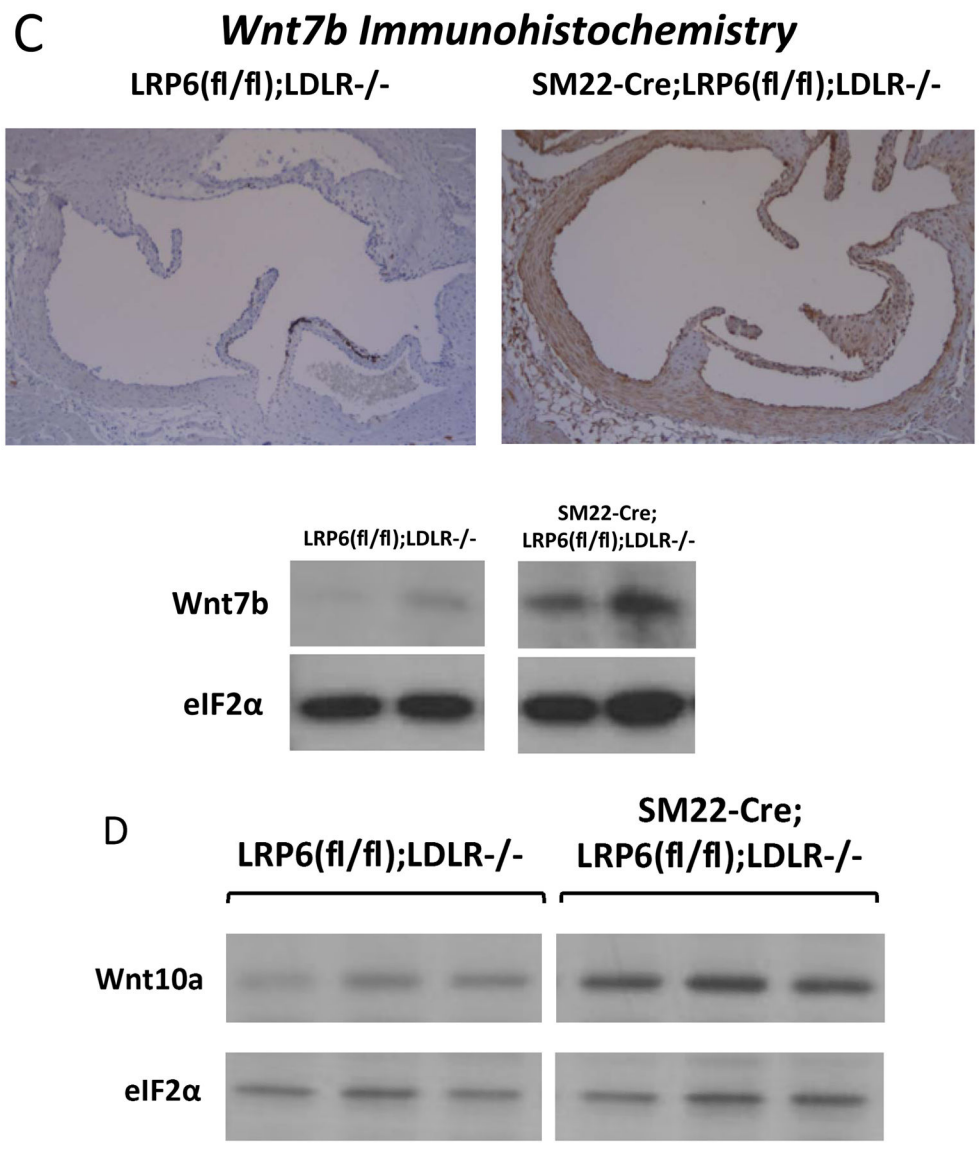

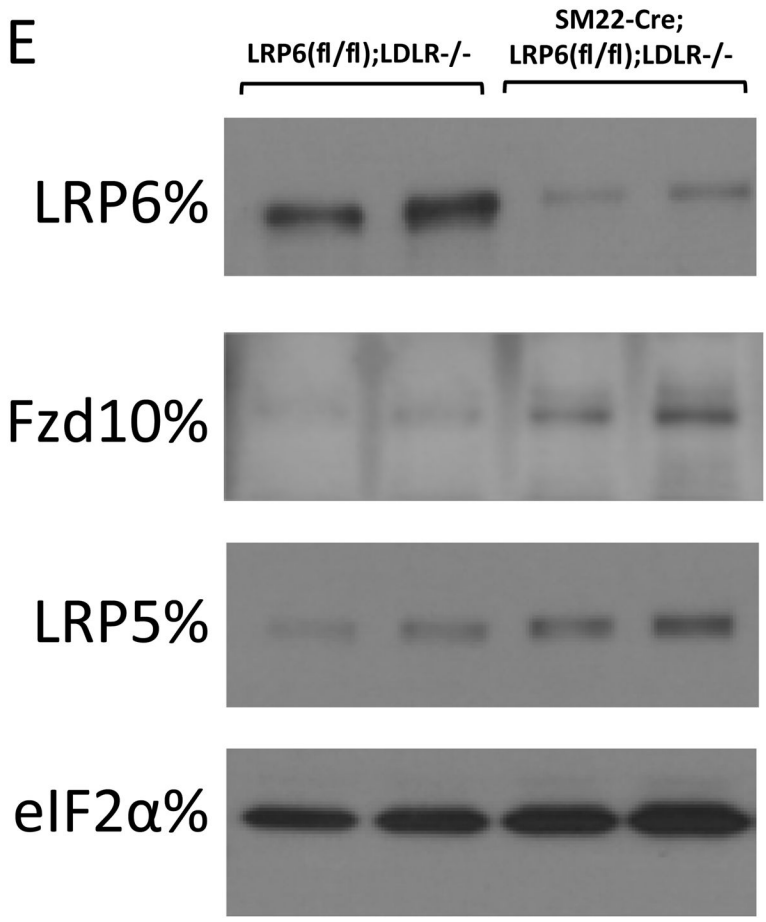

Figure 2. Wnt ligands and Fzd receptors capable of activating noncanonical signals are upregulated in aortas of SM22-Cre;LRP6(fl/fl);LDLR-/- mice fed diabetogenic diets

Panel A, RT-qPCR confirms upregulation of Wnt10a, Wnt7b, Wnt4, and Wnt3a in aortas of diabetic *SM22-Cre;LRP6(fl/fl);LDLR-/-* mice. N = 4 to 7 per group as indicated in the legend. **, $p < 0.01$ vs. Cre-negative control. ***, $p < 0.001$ vs. Cre-negative control by Student's 2-tail t-test. Panel B, the expression of Fzd10 was selectively increased, consistent with array analyses (Figure S14). ***, $p < 0.001$ vs. Cre-negative control by Student's 2-tail t-test. Panel C upper, immunohistochemistry revealed increases in aortic Wnt7b protein. Western blots using extracts from LRP6(fl/fl);LDLR-/- control and SM22-Cre;LRP6(fl/fl);LDLR-/- VSM confirmed increases in Wnt7b protein with LRP6 deficiency (lower panel). Panel D, western blot for Wnt10a protein accumulation followed by digital image analysis confirmed 3-fold upregulation of Wnt10a protein in LRP6-deficient aortic VSM ($p < 0.05$). Panel E, Cre-dependent reductions in LRP6 were accompanied by increased Fzd10 protein accumulation, consistent with analyses of whole aorta RNA (panel B above) and cultured VSM (Figure XVI).

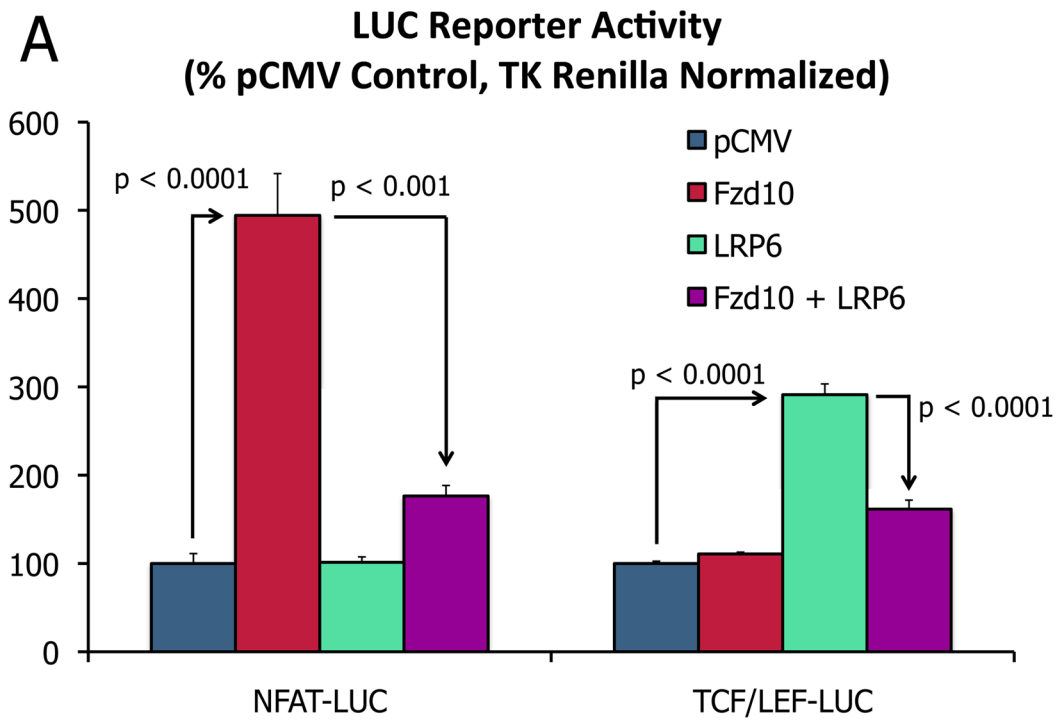

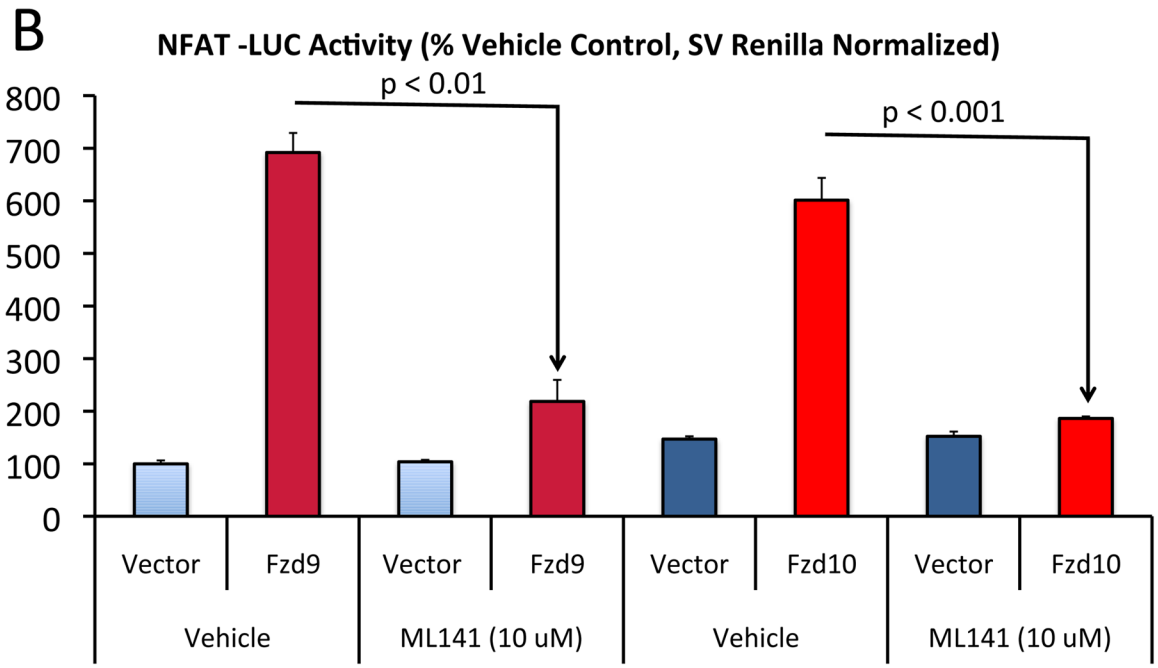

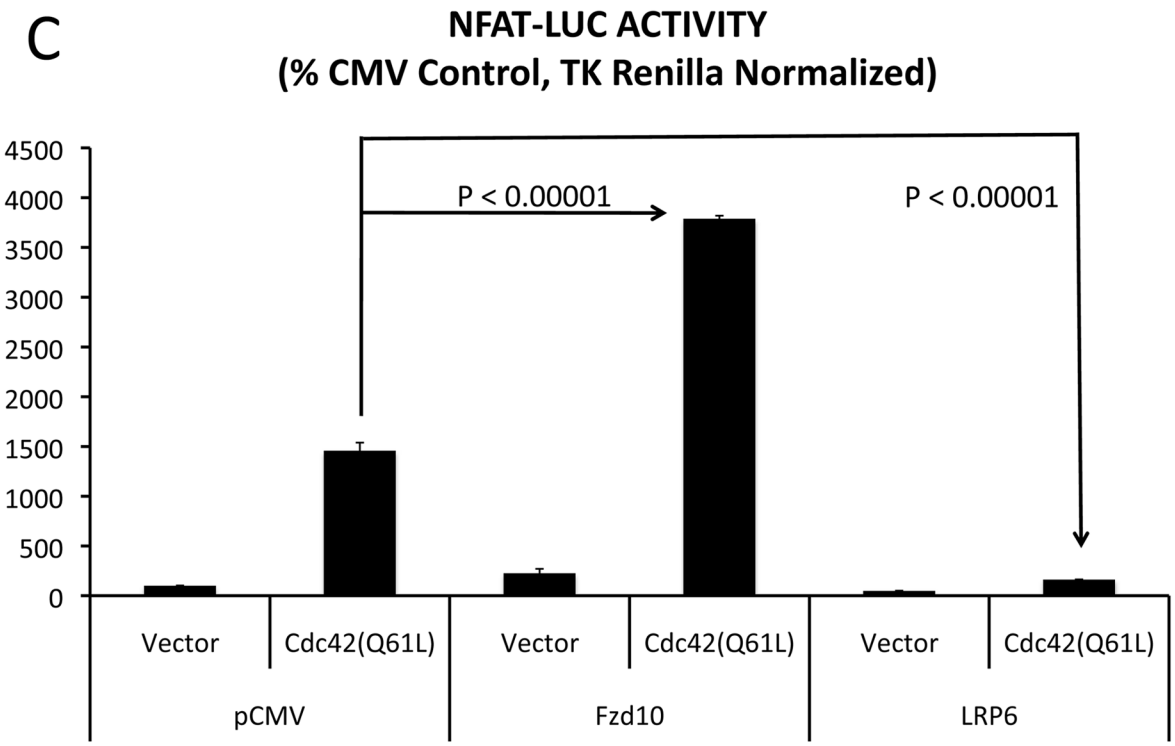

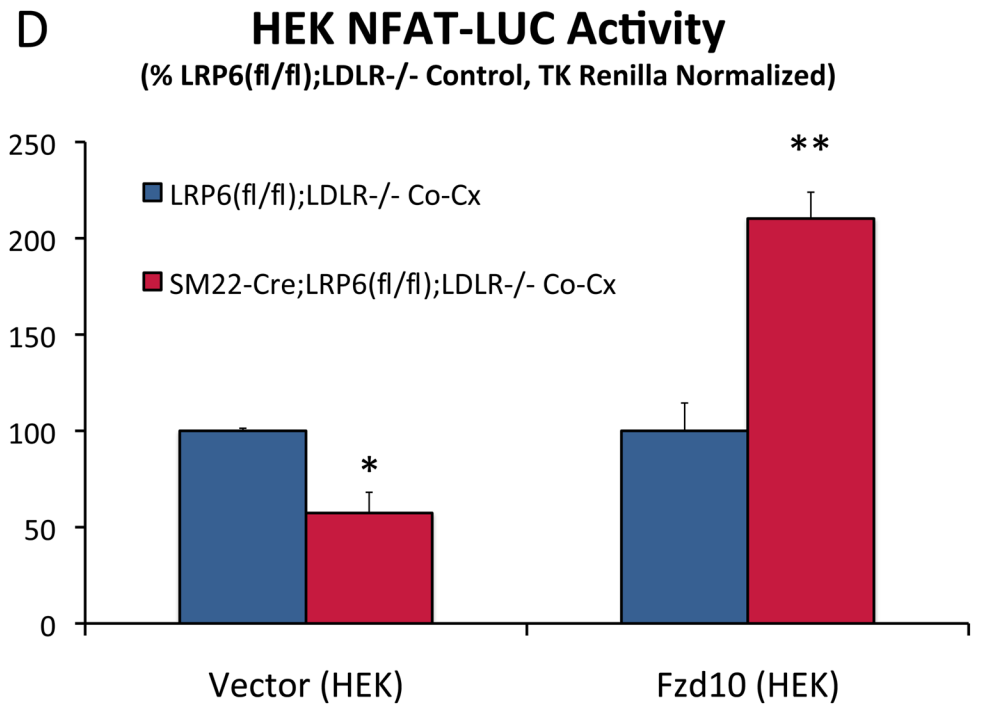

Figure 3. Fzd10 activation of noncanonical signaling is inhibited by LRP6 and the cdc42 antagonist ML141

Panel A, Fzd10 activates NFAT-LUC reporter activity in HEK cells and co-expression of LRP6 inhibits induction (left). By contrast, LRP6 activates canonical TCF/LEF signaling via

pathways inhibited by Fzd10 (right). ANOVA p <0.0001 with post-hoc Holm-Sidak testing. N = 3 per group. Panel B, ML141, a cdc42 antagonist, inhibits Fzd9 and Fzd10 induction of NFAT-LUC. Fzd1, Fzd2, and Fzd6 were inactive (not shown). ANOVA p <0.0001 with post-hoc Holm-Sidak testing. N = 6 per group. Panel C, constitutively active cdc42(Q61L) stimulation of noncanonical NFAT signaling is enhanced by Fzd10 and inhibited by LRP6. ANOVA p <0.0001 with post-hoc Holm-Sidak testing. N = 3 – 9 per group. Panel D, HEK cells were transfected with either pCMV vector + NFAT-LUC or pCMV-Fzd10 + NFAT-LUC, then parachuted for co-culture (Co-Cx) onto lawns of either LRP6(fl/fl);LDLR-/- VSM or SM22-Cre;LRP6(fl/fl);LDLR-/- VSM. Note that SM22-Cre;LRP6(fl/fl);LDLR-/- cells supported Fzd10-dependent activation of NFAT-LUC signaling, indicating enhanced elaboration of a noncanonical agonist with VSM LRP6 deficiency. ANOVA p < 0.0001, with post-hoc Holm-Sidak testing. N = 6 per group.

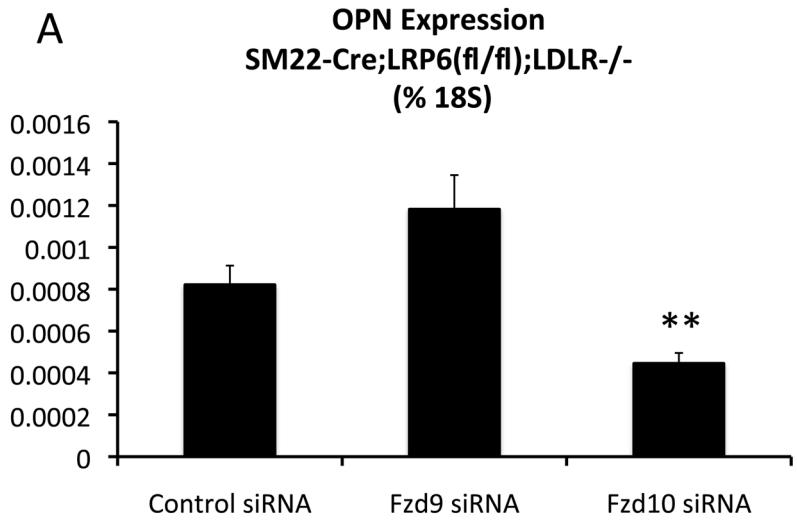

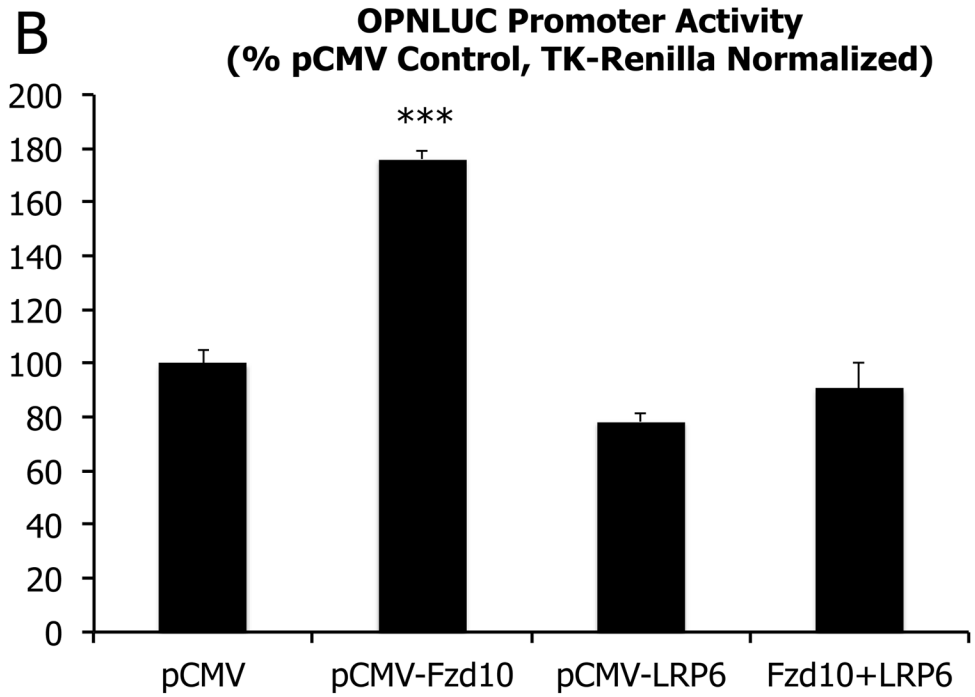

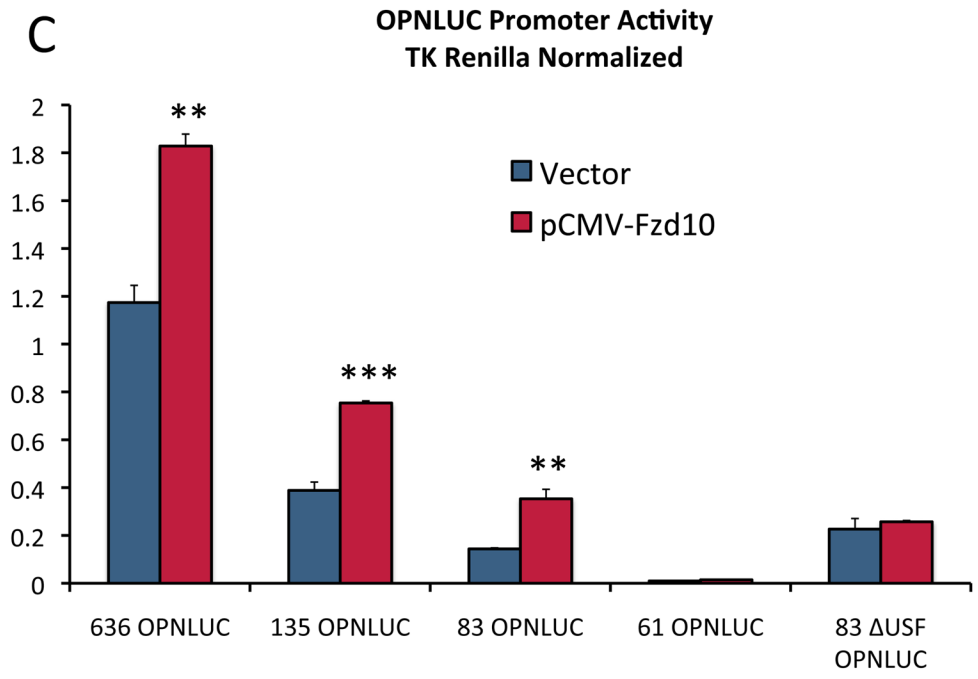

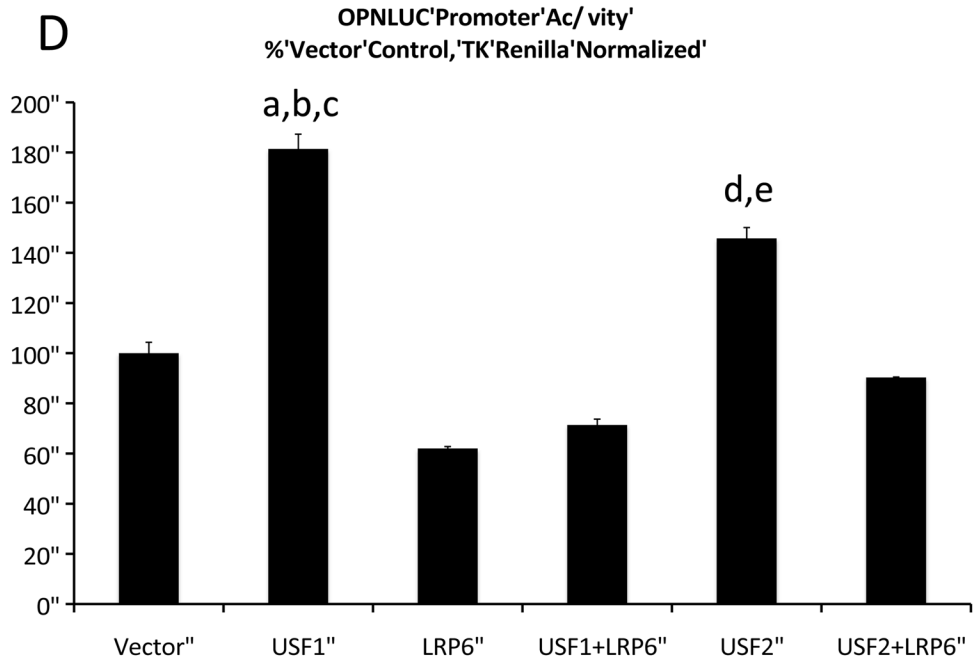

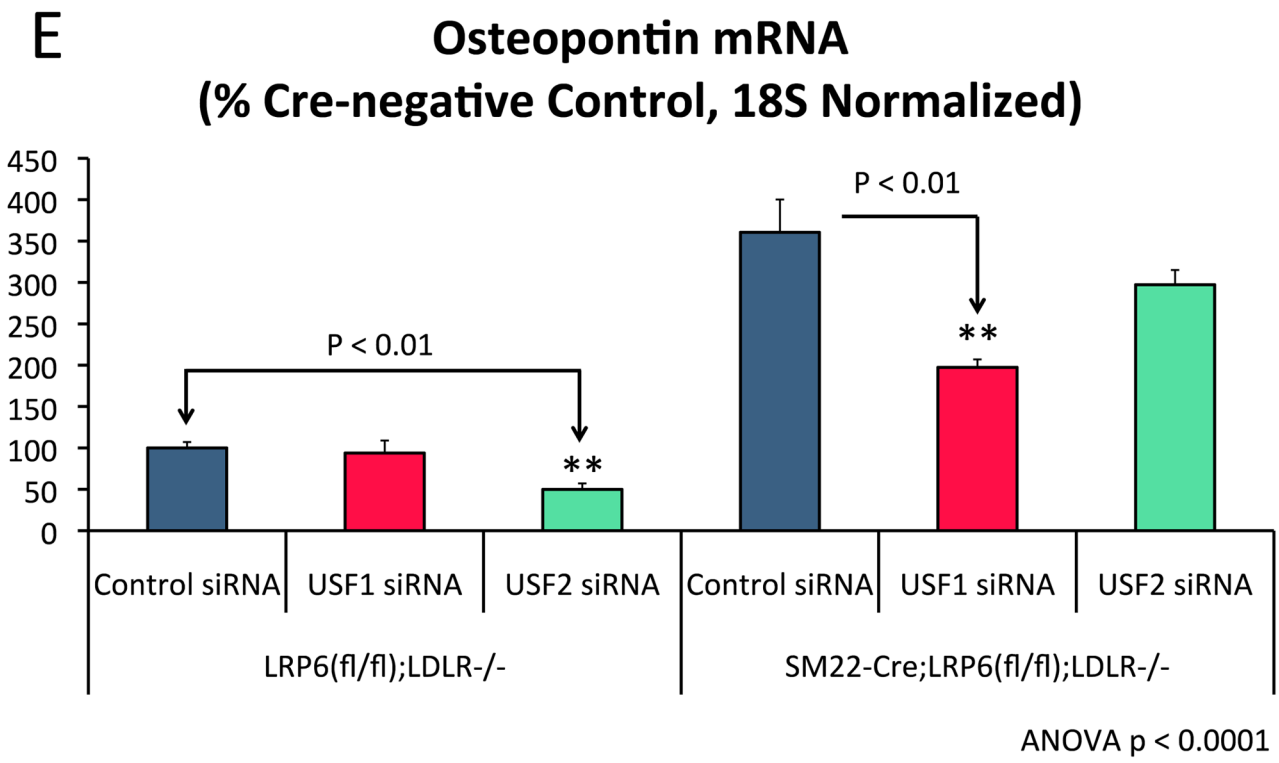

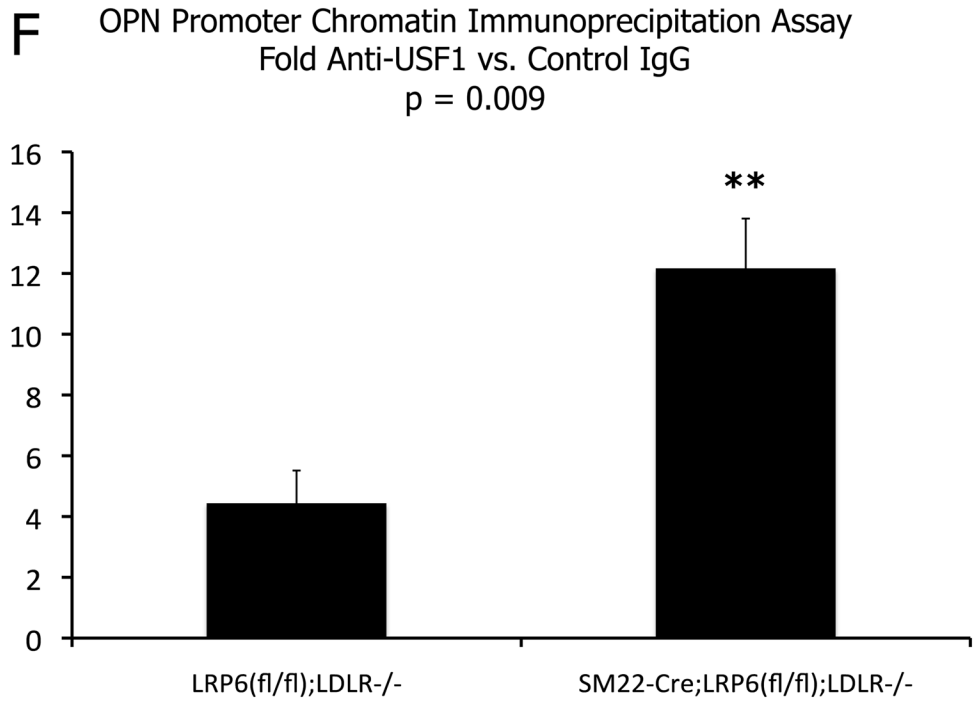

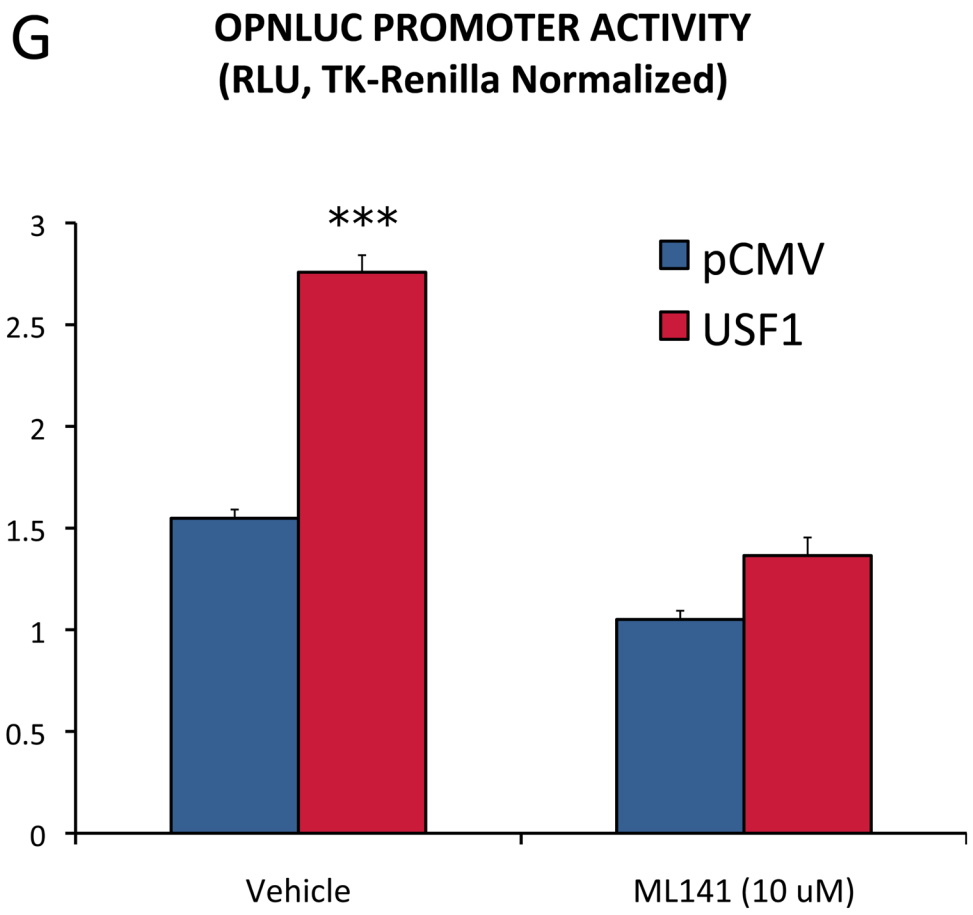

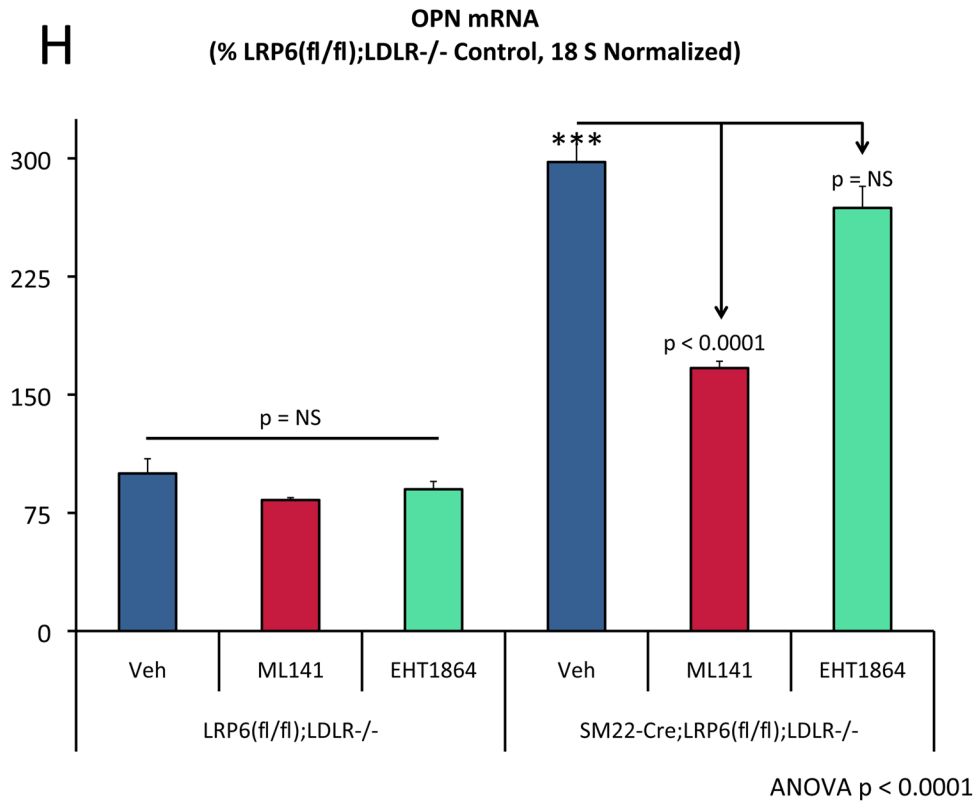

Figure 4. Fzd10 activation of OPN transcription maps to the USF cognate, and USF1 upregulation of OPN promoter activity is inhibited by LRP6 or the cdc42 antagonist ML141

Panel A, siRNA targeting Fzd10 reduced OPN expression in SM22-Cre;LRP6(fl/fl);LDLR-/- VSM. ANOVA $p = 0.001$. N = 4 per group. **, $p < 0.01$ vs. Fzd9 siRNA and $p < 0.05$ vs. control siRNA by Holm-Sidak post-hoc testing. Panel B, like NFAT-LUC, Fzd10 activation of the OPN promoter is inhibited by LRP6 expression. N = 3 per group, ANOVA $p < 0.001$; ***, $p < 0.001$ vs. all other conditions by Holm-Sidak test. Panel C, Fzd10 activation of the OPN promoter maps to the proximal CCTCATGAC USF cognate. N = 3 per group, significance assessed by Student's 2-tail t-test. Panel D, USF activation of the OPN promoter is inhibited by LRP6 expression. N =3–6 per group. ANOVA $p < 0.0001$. a, $p < 0.05$ vs. vector, b, $p < 0.001$ vs LRP6; $p < 0.01$ vs. USF1+LRP6; d, $p < 0.05$ vs. vector, e, $p < 0.02$ vs. USF2+LRP6 by Holm-Sidak post-hoc test. Panel E, USF1 siRNA, but not USF2 siRNA, significantly reduces OPN induction with LRP6 deficiency in VSM. ANOVA $p < 0.0001$, with post-hoc Holm-Sidak testing. N = 4 per group. Panel F, ChIP assay confirms increased association of USF1 with OPN chromatin in SM22-Cre;LRP6(fl/fl);LDLR-/- VSM. N = 4 per group; **, $p \leq 0.01$ by Student's 2-tail t-test. Panel G, USF1 activation of OPN promoter activity is inhibited by ML141. ANOVA $p < 0.0001$, ***, $p < 0.001$ by Holm-Sidak testing. N = 6 per group. Panel H, the increased OPN gene expression in SM22-Cre;LRP6(fl/fl);LDLR-/- VSM is reduced by ML141. By contrast, the Rac1 inhibitor EHT1864 had no effect. Treatments were 10 uM for 20 hours. ANOVA $p < 0.0001$ (post hoc Holm-Sidak). N = 4 per group.

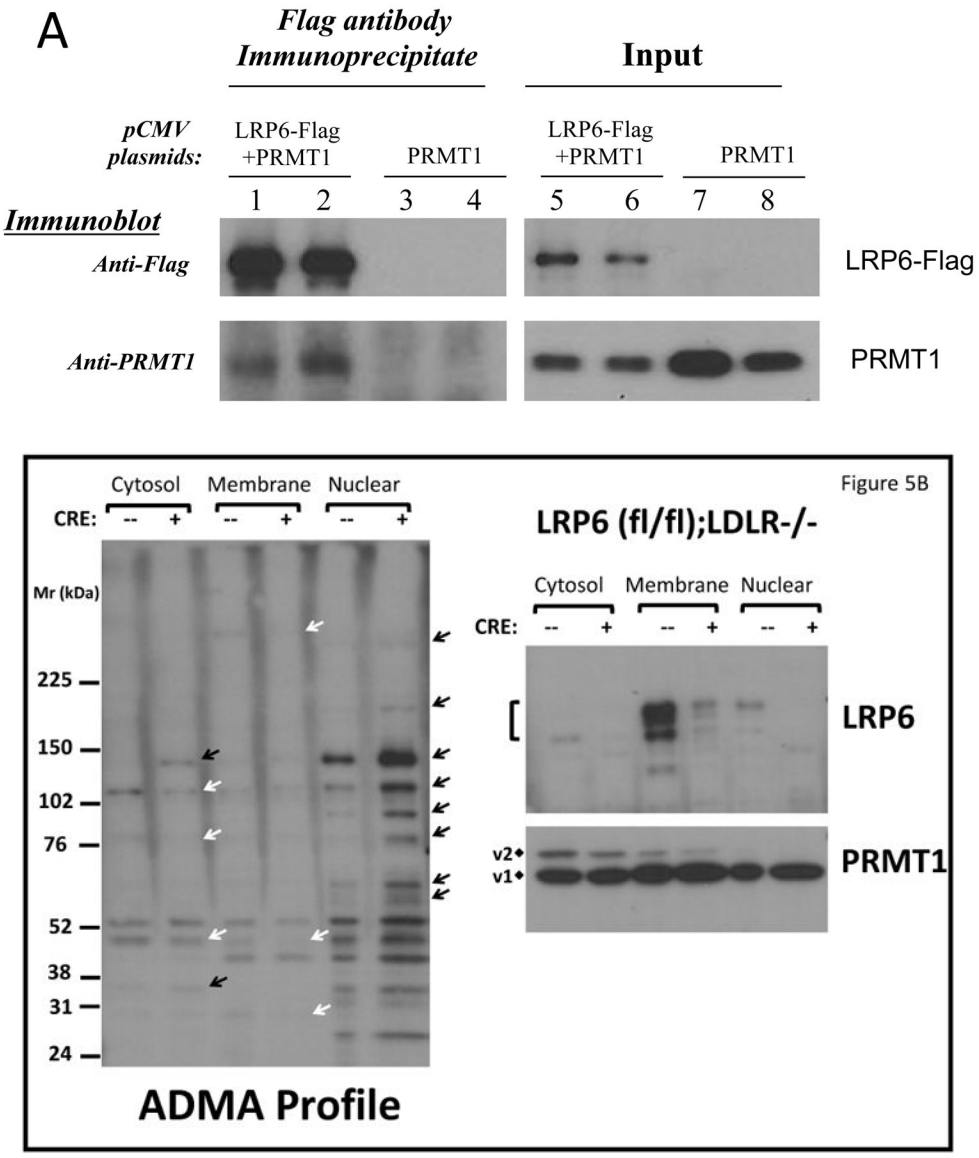

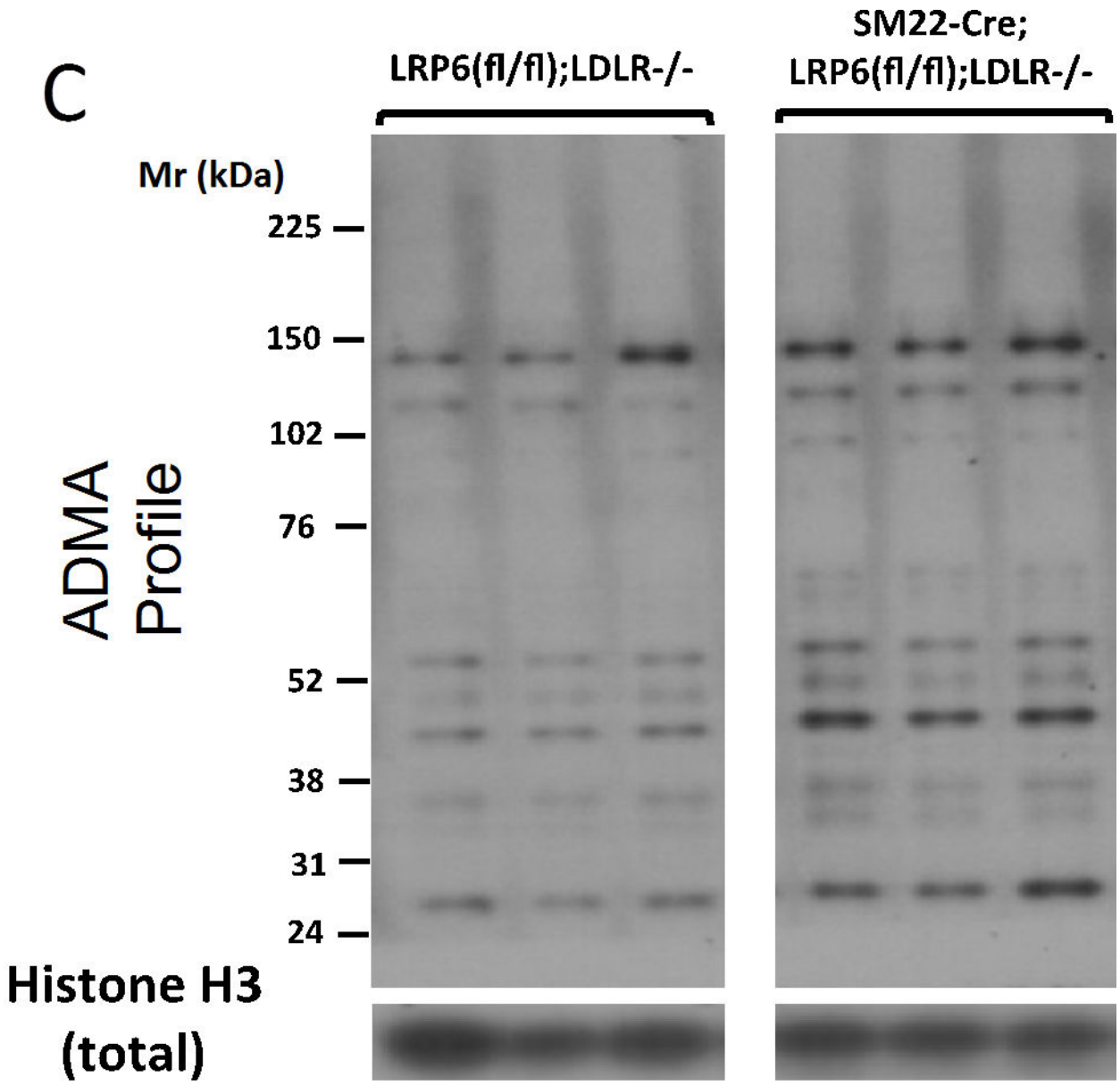

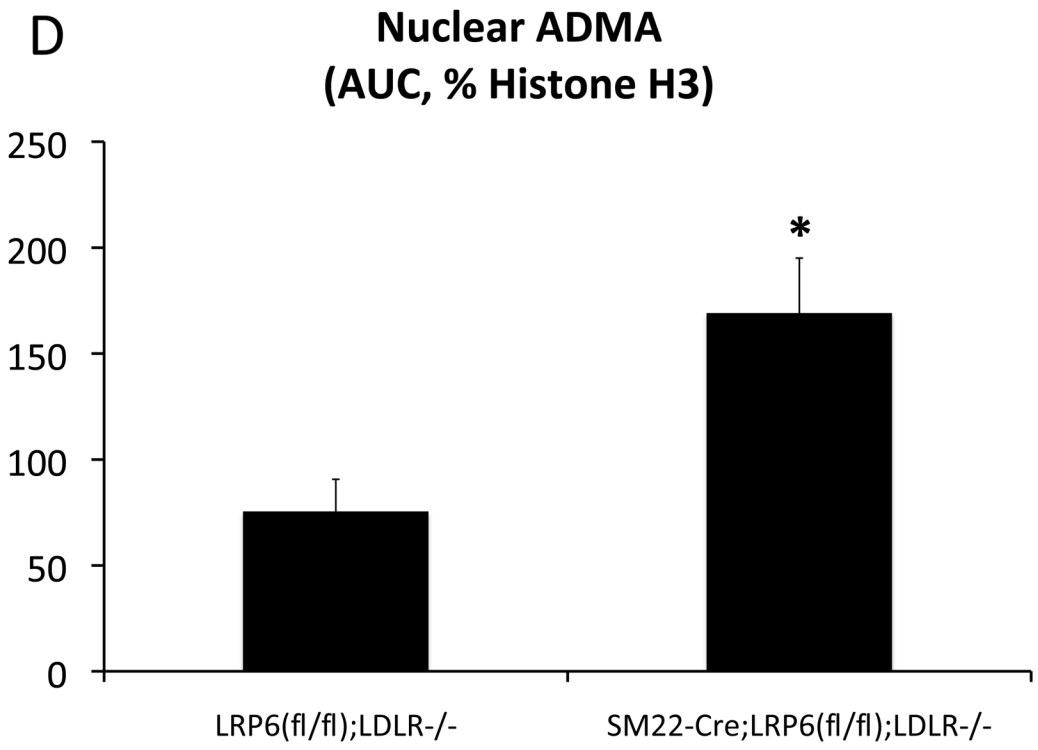

Figure 5. LRP6 forms a complex with PRMT1v1, and cellular protein ADMA accumulation is perturbed in LRP6-deficient VSM

Panel A, PRMT1v1 and Flag-tagged LRP6 are co-precipitated when co-expressed in HEK cells. Panel B left, protein asymmetric dimethylarginine (ADMA) profiles are perturbed in LRP6-deficient VSM. While a few ADMA proteins are down-regulated (white arrows), the majority of those visualized are increased in SM22-Cre;LRP6(fl/fl);LDLR-/- nuclear fraction (black arrows). Right, while Cre-mediated down-regulation of LRP6 protein in the membrane fraction was readily detected (upper right), the broad distribution of PRMT1 exhibited little if any change. v2, PRMT1 variant 2 possessing the nuclear export signal (NES). v1, PRMT1 variant 1 lacking the NES. Panels C and D, digital image analysis confirmed significant 2–3 fold increases in total nuclear ADMA protein accumulation in LRP6-deficient VSM. N = 3 per group. *, $p < 0.05$ by Student's t-test.

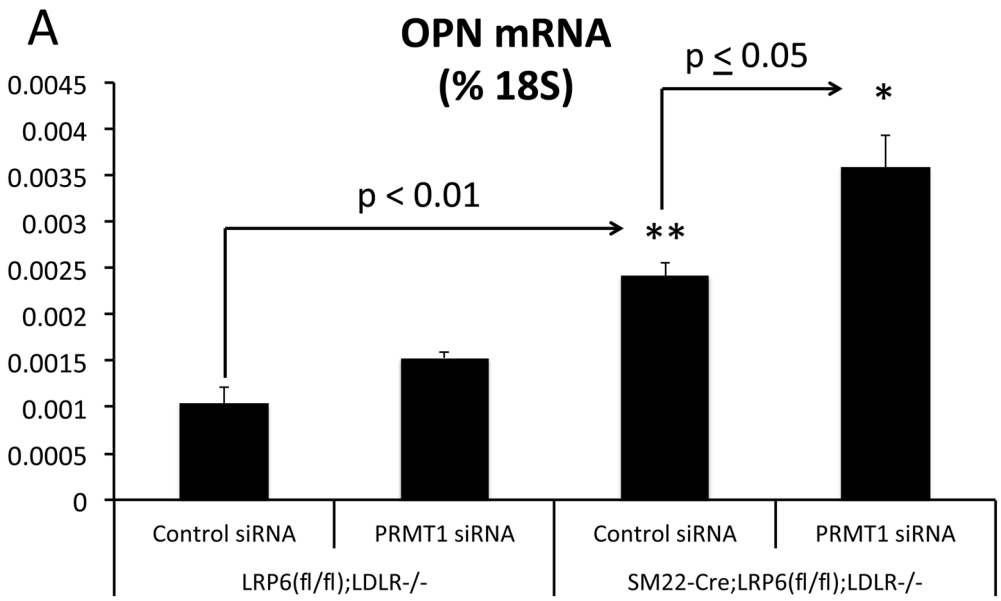

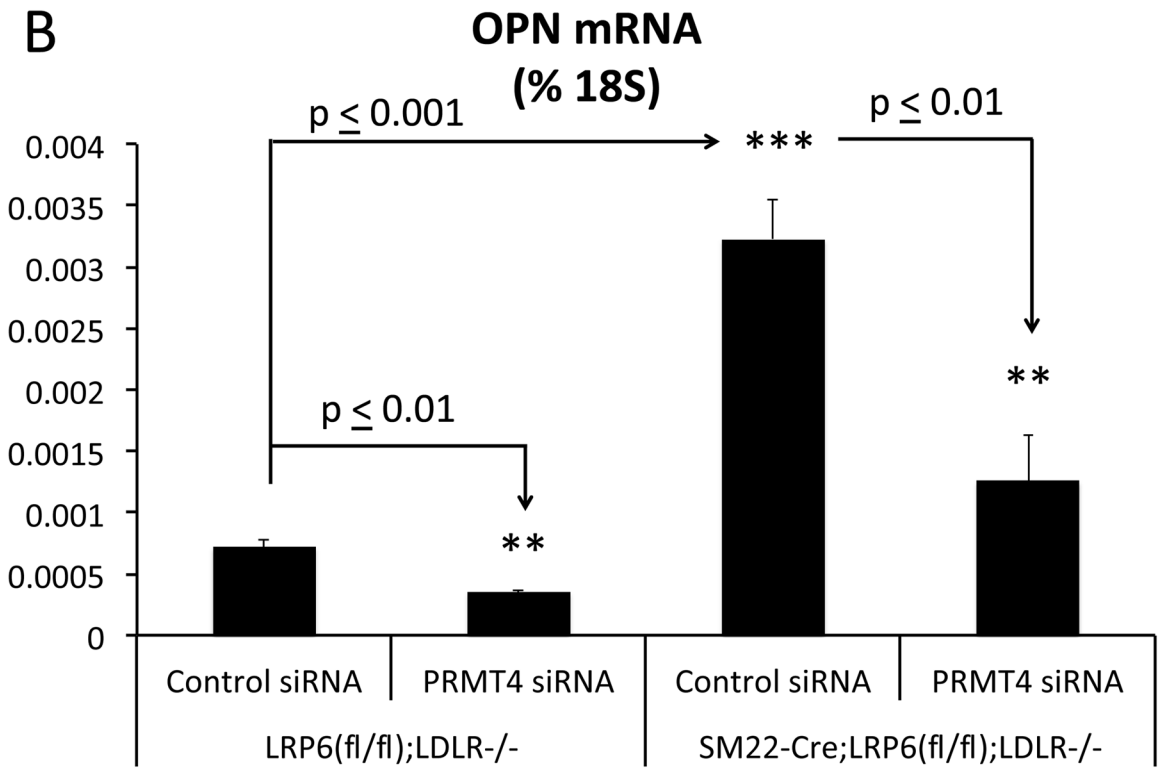

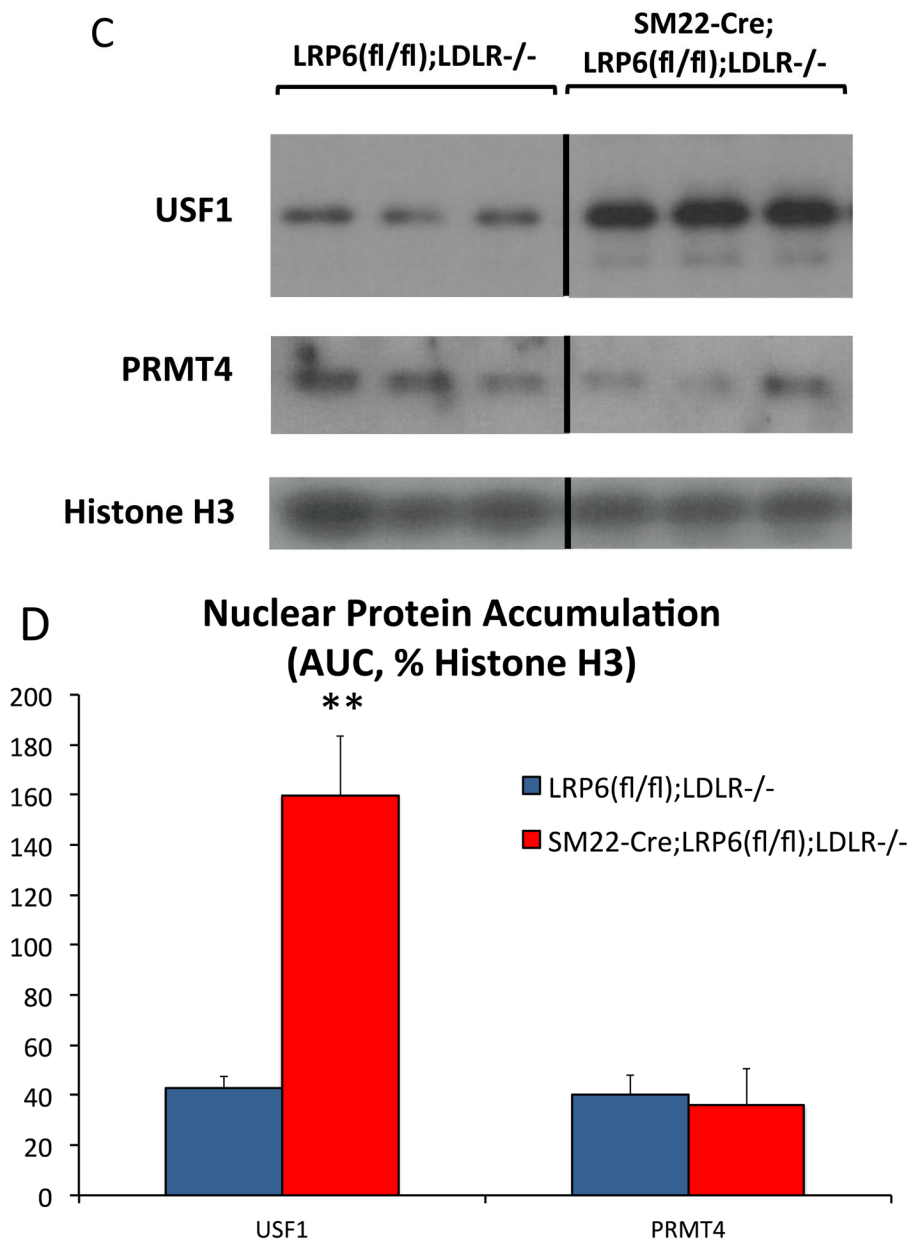

Figure 6. RNAi targeting PRMT4 reduces, while PRMT1 siRNA increases, OPN gene induction in LRP6-deficient VSM

Panel A, PRMT1 siRNA increases OPN gene expression. ANOVA $p < 0.0001$, with post-hoc testing corrected for multiple comparisons. N = 4 per group. Panel B, RNAi targeting PRMT4 almost completely inhibits induction of OPN with LRP6 deficiency. ANOVA $p < 0.0001$, N = 4 per group. Panels C and D, LRP6 deficiency increases USF1 nuclear protein accumulation without altering PRMT4. N = 3 per group. **, $p < 0.01$ by Student's t-test.

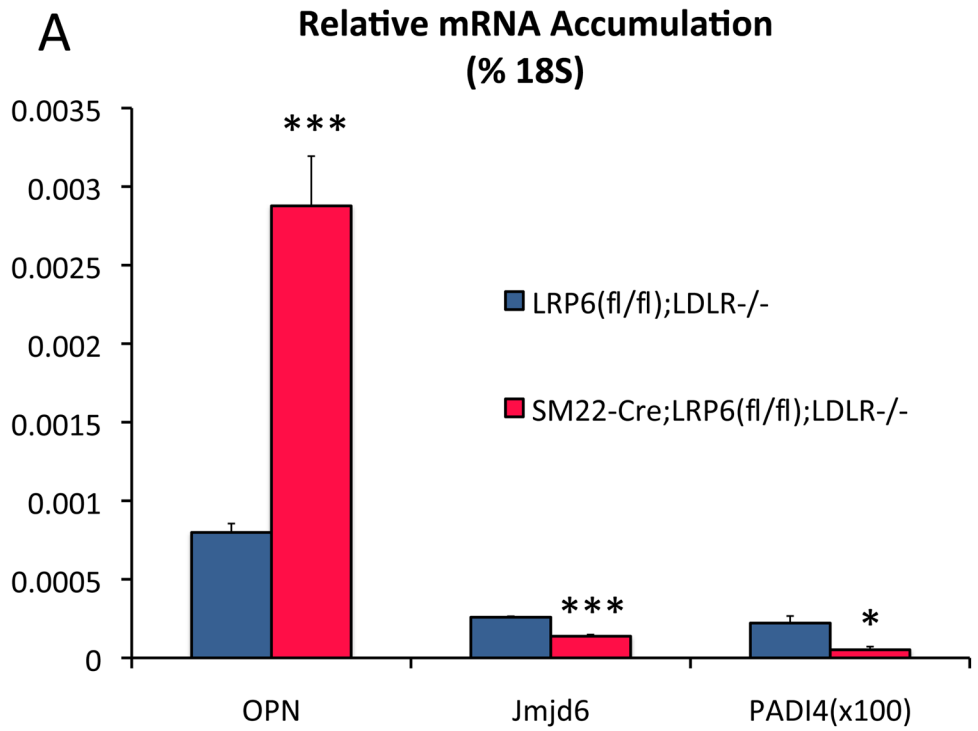

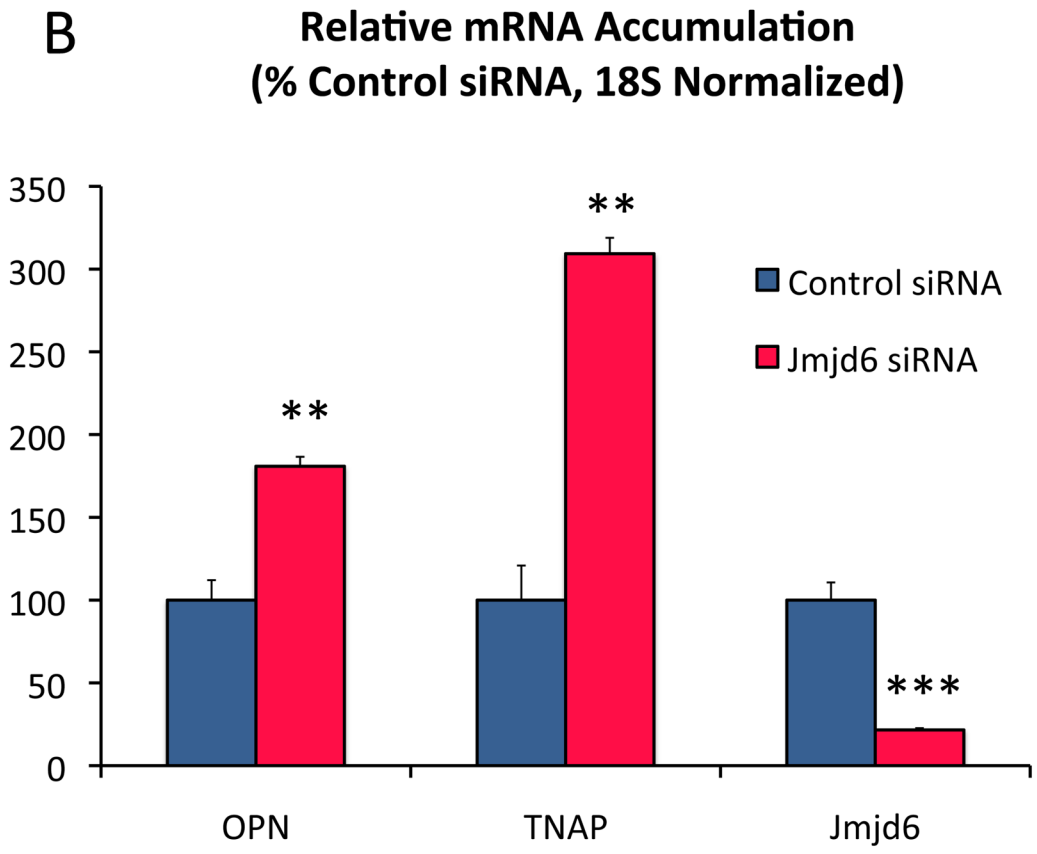

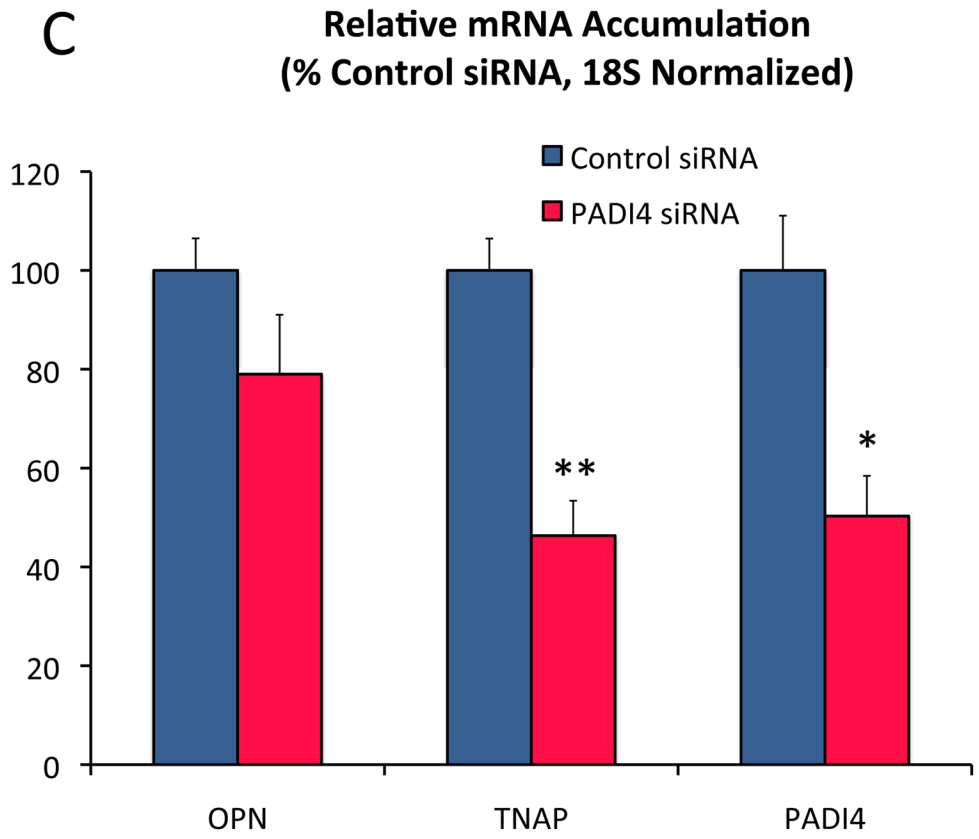

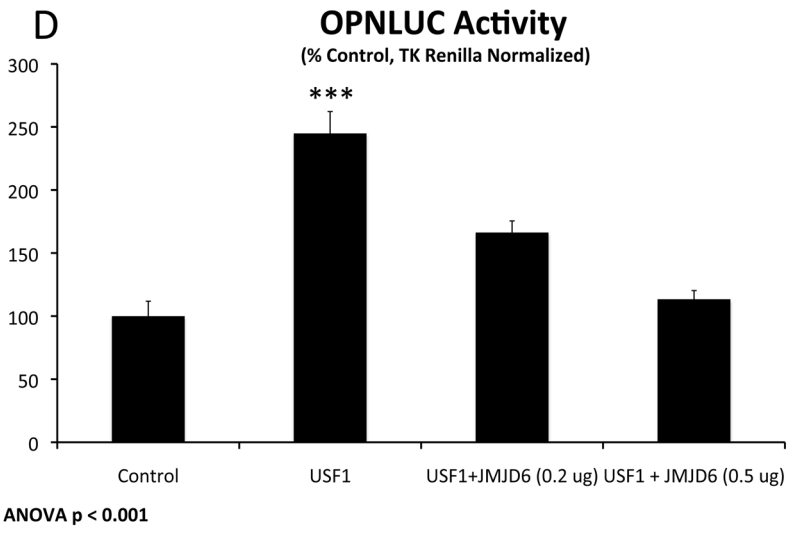

ANOVA p < 0.001

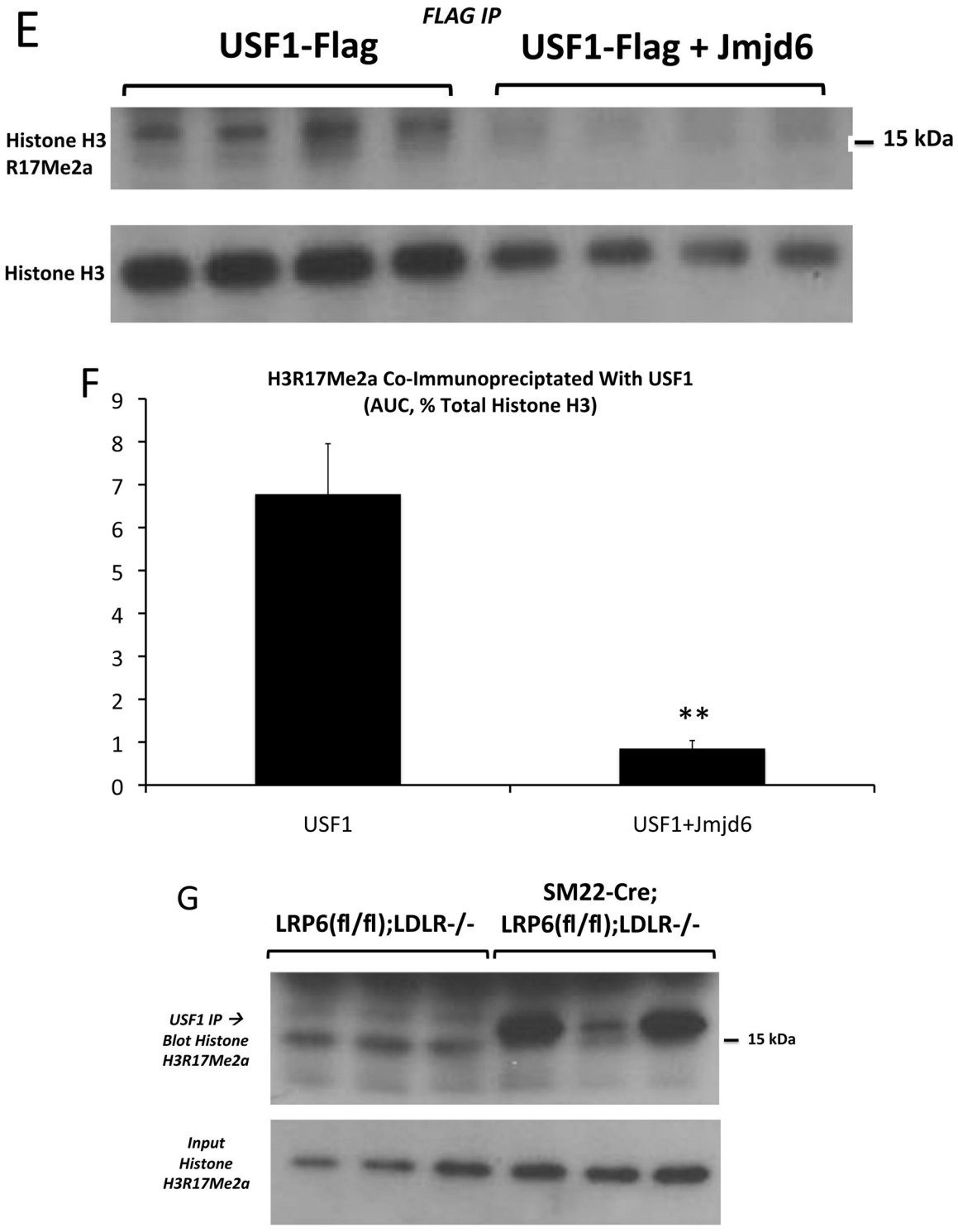

Figure 7. The broad specificity arginine demethylase Jmjd6 is reduced in LRP6 deficient VSM, restrains VSM osteochondrogenic gene expression, and inhibits USF1-dependent OPN transcription

Panel A, while *OPN* is increased with LRP6 deficiency in VSM, *Jmjd6* and *PADI4* are significantly down-regulated. The relative level of *PADI4* is ca. 100-fold less than *Jmjd6.* N

= 4 per group. *, $p < 0.05$; ***, $p < 0.001$ vs. Cre-negative control by Student's 2-tail t test. Panels B and C, *Jmjd6* siRNA significantly upregulates *OPN* and *TNAP* expression in VSM, while *PADI4* siRNA does not. N = 4 per group. **, $p < 0.01$; ***, $p < 0.001$ vs. control siRNA by Student's 2-tail t test. Panel D, Jmjd6 inhibits USF1 activation of the OPN promoter in transient transfection assays. ANOVA $p < 0.001$. ***, $p < 0.001$ vs. all other treatments by Holm-Sidak post hoc test. N = 4 per group. Panels E and F, H3 co-precipitates with Flag-tagged USF1. Co-expression of Jmjd6 significantly reduces the PRMT4 H3R17Me2a signature on histone H3 co-precipitating with USF1. N = 4 per group, $p < 0.01$ by Student's 2-tail t test. Panel G, USF1 immunoprecipitates from LRP6-deficient VSM cultures contain histone H3 bearing the PRMT4 signature H3R17Me2a.

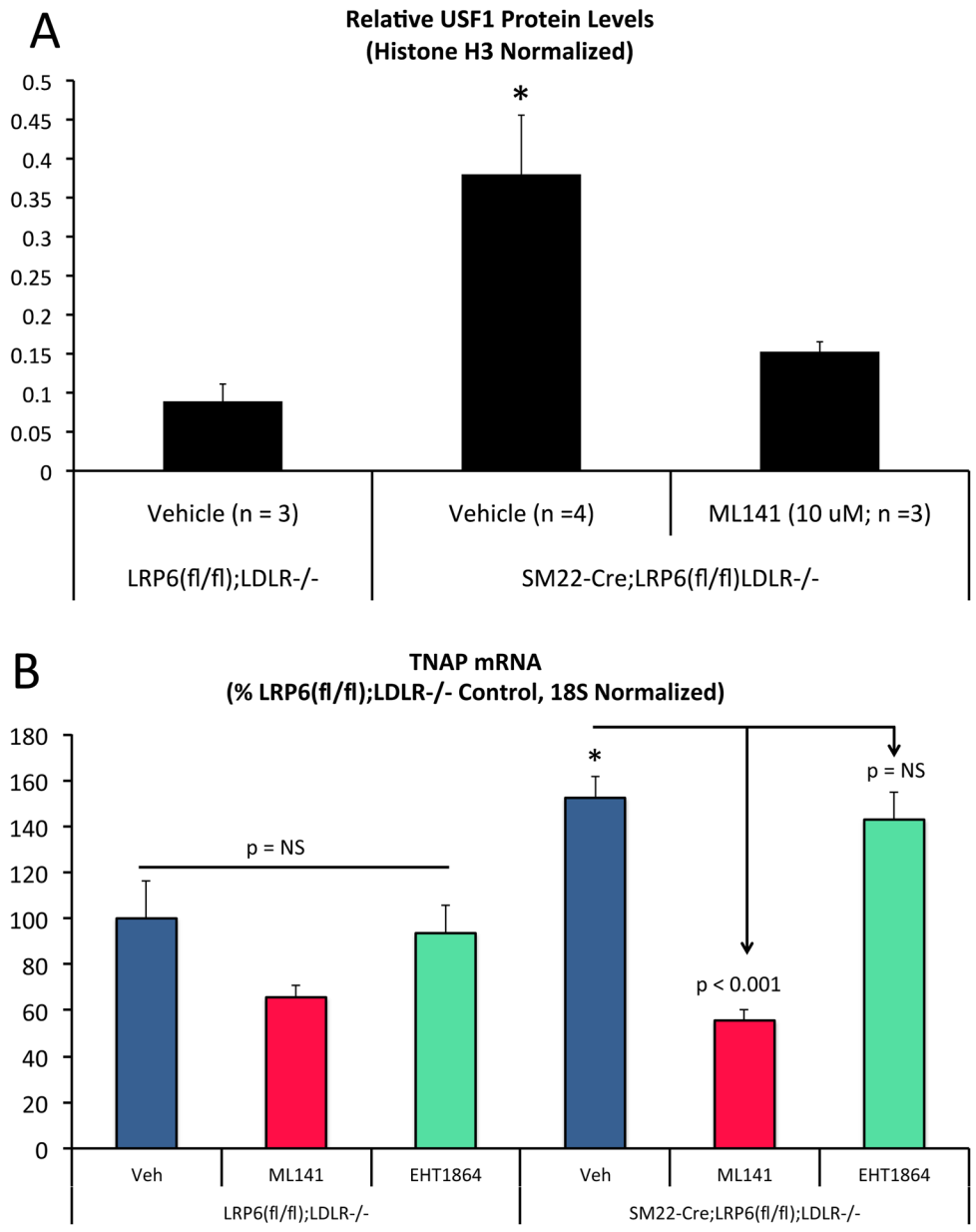

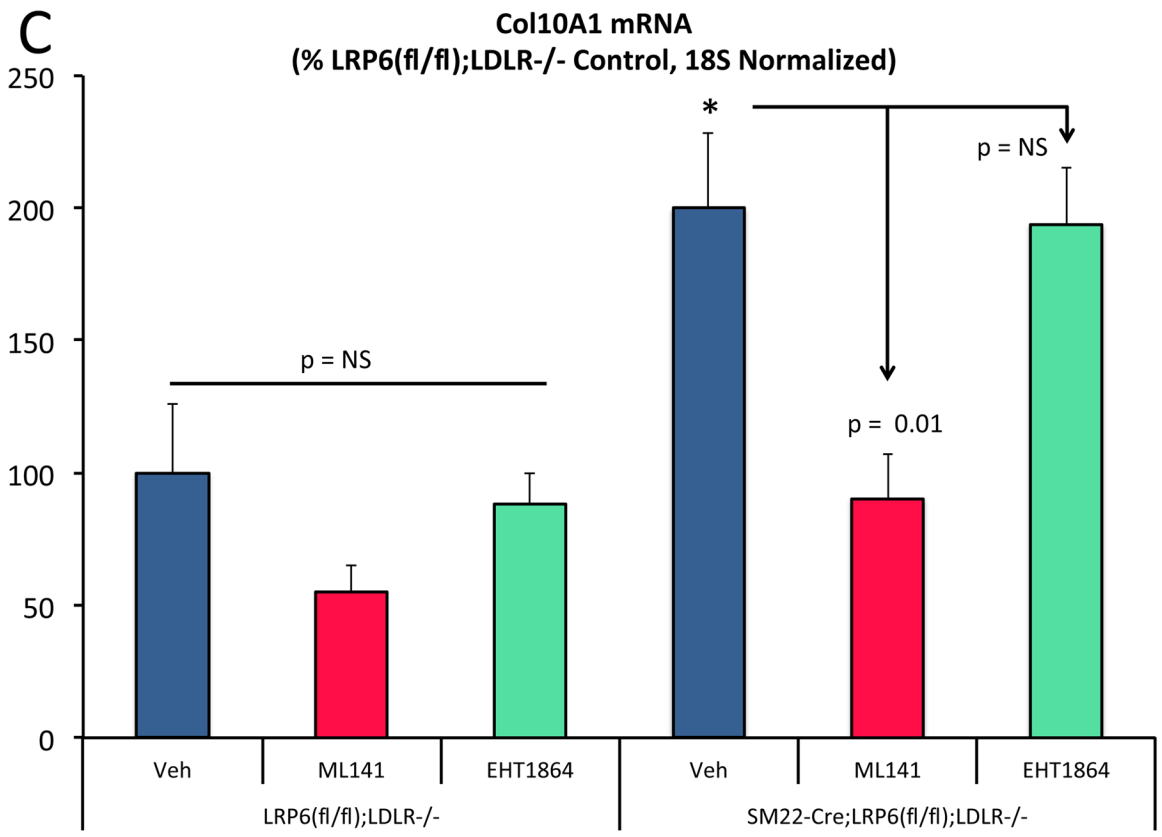

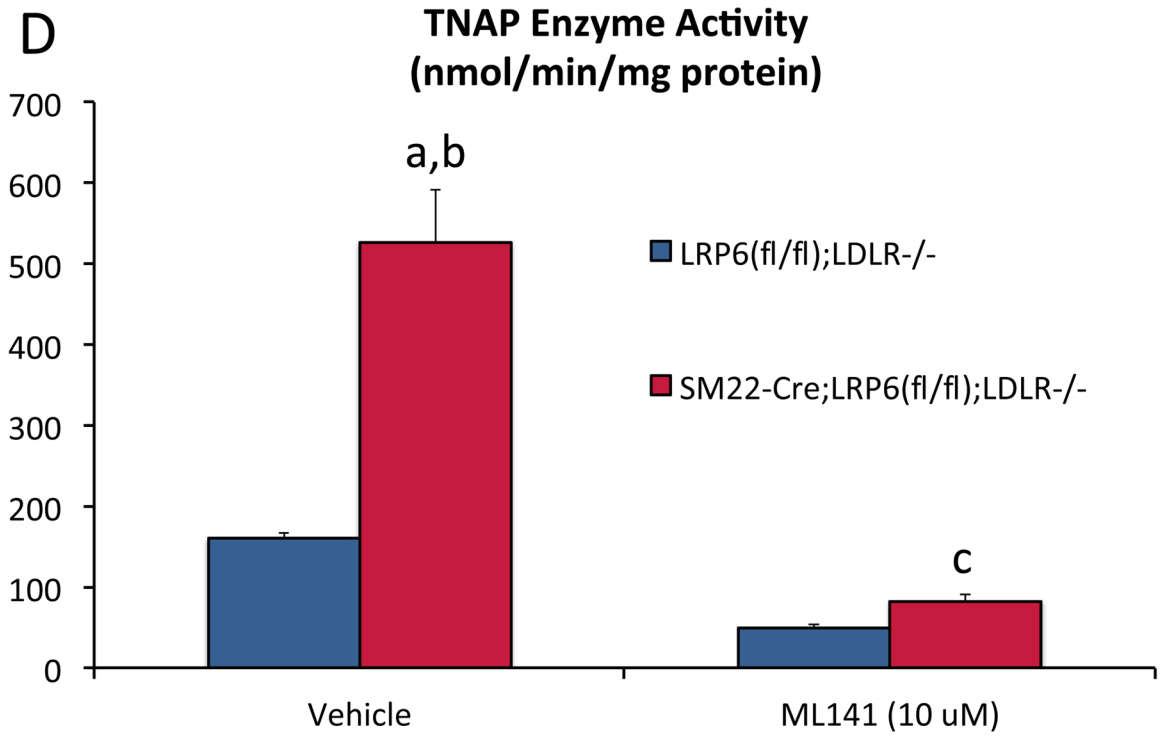

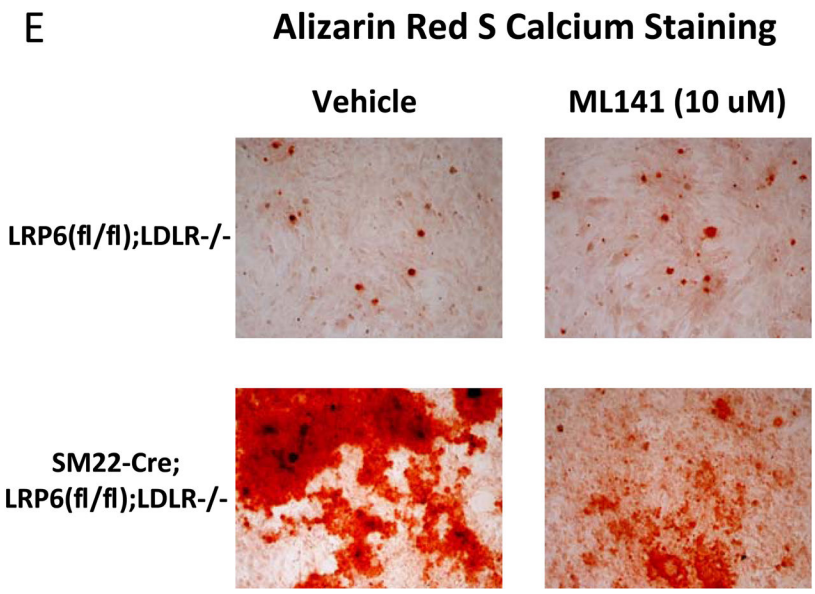

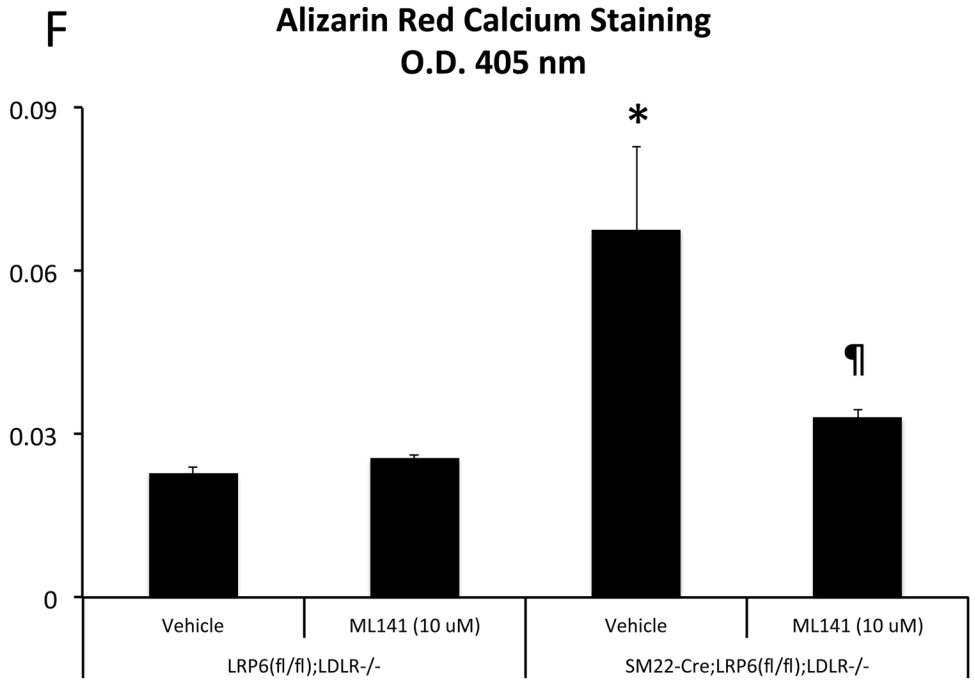

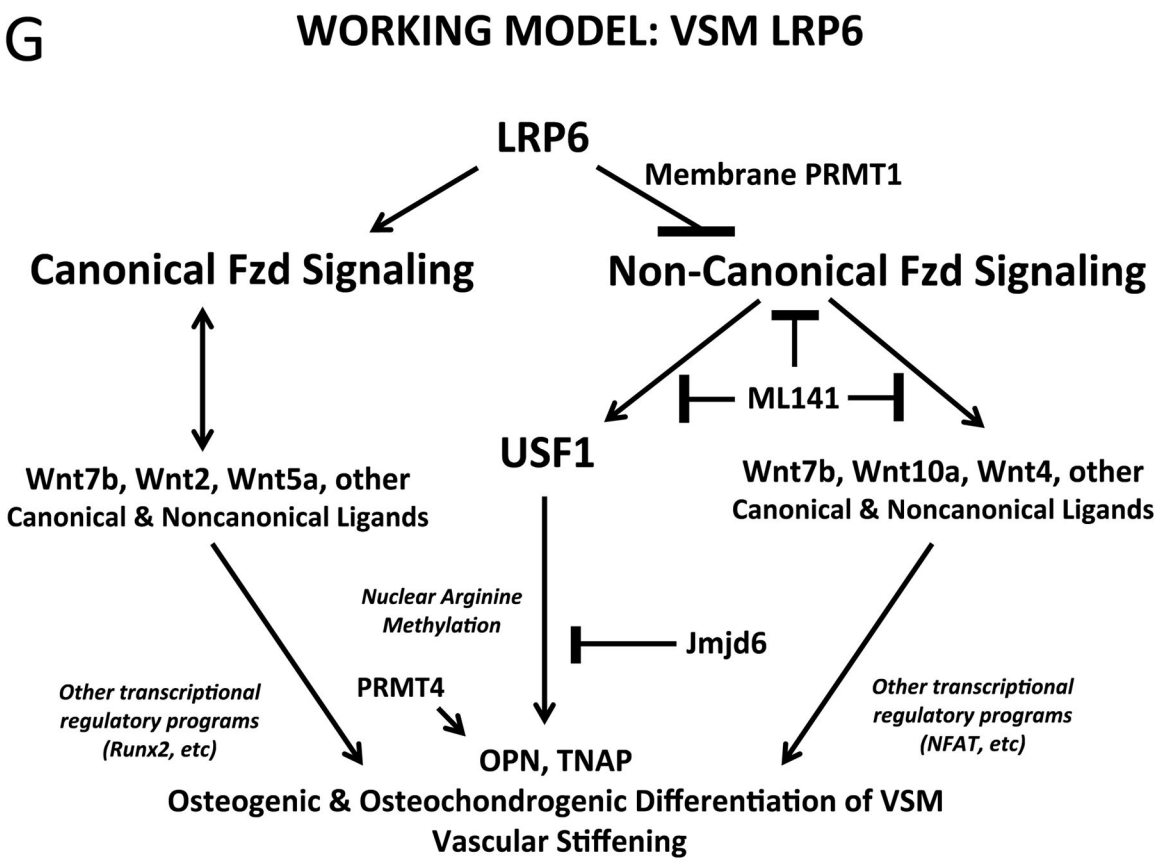

Figure 8. The cdc42 antagonist ML141 down-regulates USF1 protein accumulation and osteochondrogenic mineralization of LRP6-deficient VSM without globally altering ADMA protein profiles

Panel A, the increased VSM nuclear USF1 protein levels arising from LRP6 deficiency is reduced by ML141 treatment. Although select nuclear ADMA proteins were reduced, the global ADMA profile was largely unaffected (Figure S26 and data not shown), ANOVA $p = 0.015$, *, $p < 0.01$ from others (Holm-Sidak). N = 3–4 per group as indicated. Panels B and C, like OPN, the increases in TNAP and Col10A1 arising from LRP6 deficiency are inhibited by ML141 but not by EHT1864. *, $p < 0.05$ vs. vehicle-treated LRP6(fl/fl);LDLR-/- control. *, $p < 0.05$ vs. vehicle-treated LRP6(fl/fl);LDLR-/- control by post-hoc testing. N = 4 per group. Panel D, TNAP enzyme activity is induced with LRP6 deficiency and inhibited by ML141. ANOVA $p < 0.001$. a, $p < 0.01$ vs. vehicle treated LRP6(fl/fl);LDLR-/- control. b, $p < 0.0001$ vs. ML141 treated LRP6(fl/fl);LDLR-/- control; c, $p < 0.0001$ vs. vehicle treated SM22-Cre;LRP6(fl/fl);LDLR-/- VSM by the Holm-Sidak's multiple comparisons test. Panels E and F, Alizarin red staining of demonstrates that the increased calcification arising in SM22-Cre;LRP6(fl/fl);LDLR-/- VSM is reversed by ML141. ¶, $p < 0.05$ vs. vehicle SM22-Cre;LRP6(fl/fl);LDLR-/- VSM. N = 3 per group, ANOVA $p = 0.011$ with post-hoc Holm-Sidak's testing. Panel G, working model. See Online Supplement Figure XXX for details.